This article was downloaded by: [NASA Goddard Institute for Space Studies]
On: 23 April 2013, At: 07:23
Publisher: Taylor & Francis
Informa Ltd Registered in England and Wales Registered Number: 1072954 Registered office: Mortimer House, 37-41 Mortimer Street, London W1T 3JH, UK

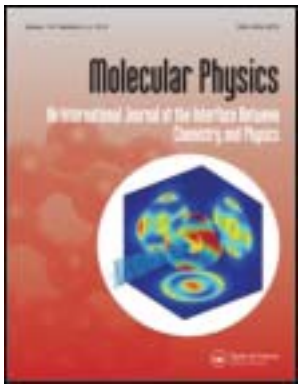

Molecular Physics: An International Journal at the Interface Between Chemistry and Physics

Publication details, including instructions for authors and subscription information:
http://www.tandfonline.com/loi/tmph20

Theoretical studies of N_2-broadened half-widths of H_2O lines involving high j states

Q. Ma [a] , R.H. Tipping [b] & N.N. Lavrentieva [c]

[a] NASA/Goddard Institute for Space Studies and Department of Applied Physics and Applied Mathematics, Columbia University, 2880 Broadway, New York, NY 10025, USA

[b] Department of Physics and Astronomy, University of Alabama, Tuscaloosa, AL 35487-0324, USA

[c] V.E. Zuev Institute of Atmospheric Optics SB RAS, 1, Akademician Zuev square, Tomsk 634021, Russia

Accepted author version posted online: 07 Dec 2011.Version of record first published: 14 Feb 2012.

To cite this article: Q. Ma , R.H. Tipping & N.N. Lavrentieva (2012): Theoretical studies of N_2-broadened half-widths of H_2O lines involving high j states, Molecular Physics: An International Journal at the Interface Between Chemistry and Physics, 110:6, 307-331

To link to this article: http://dx.doi.org/10.1080/00268976.2011.646333

PLEASE SCROLL DOWN FOR ARTICLE

Full terms and conditions of use: http://www.tandfonline.com/page/terms-and-conditions

This article may be used for research, teaching, and private study purposes. Any substantial or systematic reproduction, redistribution, reselling, loan, sub-licensing, systematic supply, or distribution in any form to anyone is expressly forbidden.

The publisher does not give any warranty express or implied or make any representation that the contents will be complete or accurate or up to date. The accuracy of any instructions, formulae, and drug doses should be independently verified with primary sources. The publisher shall not be liable for any loss, actions, claims, proceedings, demand, or costs or damages whatsoever or howsoever caused arising directly or indirectly in connection with or arising out of the use of this material.

Molecular Physics
Vol. 110, No. 6, 20 March 2012, 307–331

Taylor & Francis
Taylor & Francis Group

RESEARCH ARTICLE

Theoretical studies of N_2-broadened half-widths of H_2O lines involving high *j* states

Q. Ma[a]*, R.H. Tipping[b] and N.N. Lavrentieva[c]

[a]*NASA/Goddard Institute for Space Studies and Department of Applied Physics and Applied Mathematics, Columbia University, 2880 Broadway, New York, NY 10025, USA;* [b]*Department of Physics and Astronomy, University of Alabama, Tuscaloosa, AL 35487-0324, USA;* [c]*V.E. Zuev Institute of Atmospheric Optics SB RAS, 1, Akademician Zuev square, Tomsk 634021, Russia*

(*Received 20 September 2011; final version received 21 November 2011*)

Downloaded by [NASA Goddard Institute for Space Studies] at 07:23 23 April 2013

Based on the properties of the energy levels and wave functions of H_2O states, one can categorize H_2O lines into individually defined groups such that within the same group, the energy levels and the wave functions associated with two paired lines have an identity property while those associated with different pairs have a similarity property. Meanwhile, by thoroughly analyzing processes used to calculate N_2-broadened half-widths, it was found that the 'Fourier series' of $W^{(a)}_{L_1K_1K_1'}(t; j_f\tau_f)$ and $W^{(a)}_{L_1K_1K_1'}(t; j_i\tau_i)$, and a factor $P_{222}(j_f\tau_f j_i\tau_i)$ are the key items in the Robert-Bonamy formalism to distinguish contributions to $\mathrm{Re}S_2(r_c)$ among different transitions of $j_f\,\tau_f \leftarrow j_i\,\tau_i$. However, these items are completely determined by the energy levels and the wave functions associated with their initial and final states and they must bear the latter's features as well. Thus, it becomes obvious that for two paired lines in the same group, their calculated half-widths must be almost identical and the values associated with different pairs must vary smoothly as their j_i values vary. Thus, the pair identity and the smooth variation rules are established within individual groups of lines. One can use these rules to screen half-width data listed in HITRAN and to improve the data accuracies.

Keywords: energy levels and wave functions of H_2O states; Robert-Bonamy theory; theoretically calculated half-widths and shifts; rules governing spectroscopic parameters of H_2O lines; HITRAN

1. Introduction

The modelling of the atmosphere from satellite-based, balloon-based, and Earth-based instruments requires an accurate spectroscopic database such as HITRAN [1,2]. This widely used database has spectroscopic parameters for the most important molecules in bands from the microwave to the ultraviolet spectral regions. It is obvious that the accuracy of these data is essential for users' applications. This is especially true in accurate atmospheric retrievals involving the very important water vapor molecule. In order to meet the accuracy requirement for the H_2O molecule, the H_2O database in HITRAN has been updated several times [1,2] and a new HITRAN 2012 version will appear soon. In the recent updating process, the majority of the pressure broadened half-widths, the temperature exponents, and the pressure-induced shifts come from theoretically calculated values using the Robert-Bonamy (RB) formalism [3]. It is worth mentioning that the RB formalism was developed more than three decades ago and it contains several basic assumptions whose applicability was not thoroughly justified. Mainly due to difficulties in developing better formalisms to carry out practical calculations, there are no viable alternatives available and one has to rely on the RB formalism at present. Besides, for lines with small half-width values, contributions to their calculated half-widths result mainly from nearly head-on collisions in which two interacting molecules can reach closer distances [4]. Unfortunately, the largest uncertainties in modeling interaction potentials and collision trajectories usually occur in the short distance regions and they could lead to large errors in calculating contributions from nearly head-on collisions. Thus, calculated half-width values for lines with small half-width values are less reliable [4]. Meanwhile it turns out that, in general, lines with small half-widths are those involving high *j* states. Thus, uncertainties associated with calculated values would be worse than the requirements needed for users' atmospheric applications, especially for lines with high *j* values.

On the other hand, some of the data for the water vapor lines are experimental and may come from different labs. Given the fact that lines with high *j* values are usually weak, to perform measurements for them becomes more difficult and measured results

*Corresponding author. Email: qma@giss.nasa.gov

ISSN 0026–8976 print/ISSN 1362–3028 online
© 2012 Taylor & Francis
http://dx.doi.org/10.1080/00268976.2011.646333
http://www.tandfonline.com

Downloaded by [NASA Goddard Institute for Space Studies] at 07:23 23 April 2013

could contain larger uncertainties. In addition, there are a huge number lines especially at high temperatures, and the majority of them are associated with high j states, and thus to provide these data from experimental measurements is not realistic. In summary, the current uncertainties for the half-widths in the H_2O database are far beyond the desired accuracy and it seems that this situation could last for a while.

In order to find realistic ways to improve the accuracies of half-widths of H_2O lines, we began this study by wondering whether links between lines of interest and their half-widths do exist or not. If the answer is yes, we hoped that some rules representing these links can be discovered. Of course, the success of this idea relies not only on the nature of pressure broadened half-widths, but also the answer to the fundamental question about why and how calculated N_2-broadened half-widths vary for the lines of interest. In fact, we have been interested in this fundamental question for several years and have made many efforts to search for the answer. Very recently, however, we have found a method and in the following we outline our route leading to the answer yes. Readers who are not familiar with the theory may skip over the next three paragraphs.

It is well known that calculated half-widths depend on the lines of interest and also on the environment in which the absorber molecule H_2O is immersed. In order to find the answer, our approach is to separate these two dependences as completely as possible. In theoretical calculations, the former is described by the initial and final states of H_2O and the latter is explicitly represented by the interaction potential and trajectory models. Within the RB formalism, our investigation targets are contributions to the term of $\mathrm{Re}S_2(r_c)$ from individual correlation functions because $\mathrm{Re}S_2(r_c)$ plays a crucial role in determining calculated half-widths. Along this way, we have found that for each of the correlations, both its contributions to $\mathrm{Re}S_{2,\,outer,\,i}(r_c)$ and $\mathrm{Re}S_{2,\,outer,\,f}(r_c)$, two of the components of $\mathrm{Re}S_2(r_c)$, can be expressed as integrations over time whose integrands mainly consist of two functions. One is the correlation function $F_{L_1K_1K_1'L_2}(t)$ that depends on the potential and trajectory models and is common for all lines. The other is the two functions $W^{(a)}_{L_1K_1K_1'}(t;j\tau)$ which depend on the initial or the final states of the lines of interest but are independent of the environment. Thus, for an individual line, two $W^{(a)}_{L_1K_1K_1'}(t;j\tau)$ associated with its initial and final states contains all information necessary to determine its contributions to $\mathrm{Re}S_{2,\,outer,\,i}(r_c)$ and $\mathrm{Re}S_{2,\,outer,\,f}(r_c)$. Therefore, it is these two functions $W^{(a)}_{L_1K_1K_1'}(t)$ that distinguish the different magnitudes of $\mathrm{Re}S_{2,\,outer,\,i}(r_c)$ and $\mathrm{Re}S_{2,\,outer,\,f}(r_c)$ for individual lines. Meanwhile, similar analysis can be applied to the term of $S_{2,\,middle}(r_c)$, the remaining component of $\mathrm{Re}S_2(r_c)$ also. In this case, it is a factor $P_{L_1K_1K_1'}(j_f\tau_f j_i\tau_i)$ that depends on the lines of interest but is independent of the environment. Then, we know that in order to find the answers we need to focus our attention on the two functions $W^{(a)}_{L_1K_1K_1'}(t;j\tau)$ and the factor $P_{L_1K_1K_1'}(j_f\tau_f j_i\tau_i)$.

It turns out that expressions for $W^{(a)}_{L_1K_1K_1'}(t;j\tau)$ are given in terms of 'Fourier series' and the number of their major components is very limited. This implies that each $W^{(a)}_{L_1K_1K_1'}(t;j\tau)$ can be well represented by a spectrum containing only several components. As a result, to analyze profiles of $W^{(a)}_{L_1K_1K_1'}(t;j\tau)$ among many different states becomes easier. By simply plotting distributions of the spectra associated with different H_2O states, we have found that there are identities of their distributions between certain pairs of states and there are similarities within certain groups of states also. With respect to values of $P_{L_1K_1K_1'}(j_f\tau_f j_i\tau_i)$, similar features have also been found. In addition, the events associated with $W^{(a)}_{L_1K_1K_1'}(t;j_f\tau_f)$ and $W^{(a)}_{L_1K_1K_1'}(t;j_i\tau_i)$ and the events with $P_{L_1K_1K_1'}(j_f\tau_f j_i\tau_i)$ happen simultaneously among the same lines.

Thus, we are sure that the similar features must exist for the calculated half-widths among certain lines. Armed with the knowledge where the identity and the similarity happen for $W^{(a)}_{L_1K_1K_1'}(t;j\tau)$ and $P_{L_1K_1K_1'}(j_f\tau_f j_i\tau_i)$, we know how to categorize lines into different groups. Then by checking values of the calculated half-width for lines in the same group, our expectation is well verified. At this stage, we are only one step away from finding the answer, namely. we have to explain why these features exist within the groups. Based on quantum mechanics, the energy levels and the wave functions of the H_2O states contain all information about the states. Therefore, the latter is a right place to search the answer. By investigating the properties of the energy levels and the wave functions of states, their identities and similarities clearly emerge within the groups. Thus, we have got the answers. With respect to the first question why calculated half-widths vary with the lines, it results from individual energy levels and wave functions associated with their initial and final states. Concerning the second question how calculated results vary with the lines, we know the answer within individually defined groups. It is the identities and the similarities of their energy levels and their wave functions that govern their variations.

After realizing the above, an immediate thought was that there must be similar rules valid for other spectroscopic parameters. In fact, we consider a system consisting of an absorber water molecule immersed in bath molecules while the absorber interacts with electromagnetic fields as a black box. The inputs and

Downloaded by [NASA Goddard Institute for Space Studies] at 07:23 23 April 2013

the outputs of this black box are the transition lines of H_2O and their spectroscopic parameters. The main assumptions introduced here are: (1) the outputs depend on the inputs; (2) identical inputs should yield identical outputs; and (3) similar inputs should yield similar outputs. Then, by fully exploiting the identity and similarity properties of the energy levels and wave functions, without knowing what really happens inside the black box, we can expect that the identity and similarity features exist among the spectroscopic parameters. We have found that measurements from different groups do demonstrate the above claim. In addition, several important applications have been proposed. The study based on the black box theory was summarized in a recent paper [5].

For the theoretically calculated N_2-broadened half-widths, we know completely what happens inside of the system. Instead of relying on the black box, we can establish these rules from rigorous theoretical analyses. In addition by developing tools used in the analysis, new features of the line-shape theory can be exhibited. Therefore, the present work is supplementary to recent work [5]. In the present study, we do not follow our discovery route exactly. Because properties of the energy levels and wave functions are fundamental, we first present our discussion of this subject in Section 2. With this as a guide, we then present our analysis, step by step, in the following sections. Finally, we present a short discussion and conclusion section.

2. Properties of energy levels and wave functions of H_2O

It is well known that when one studies energy levels and wave functions for an asymmetric top molecule such as H_2O, one must identify its three principal axes a, b, c with a body-fixed frame [6–9]. There are six different choices to make the identification and they are designated: I R, I L, II R, II L, III R, and III L. Of course, in describing energy levels and wave functions, all these representations are equivalent. The energy levels are independent of the choice of representation. However, the wave functions would be different, but wave functions derived from different representation are exchangeable. One can change them by using rotational transformations representing proper rotation operators under which one body-fixed frame rotates into another. In practice, one can choose the most suitable representation according to one's preference.

For years there have existed subroutines available to enable one to obtain energy levels and wave functions for important rotational states. Thus, in pursuing their spectroscopic studies, most people adopt energy levels and wave functions derived from these subroutines and they usually do not pay too much attention to these items themselves. However, it turns out that exploiting the properties of energy levels and wave functions proves to be a great help. In order to support this claim, we exhibit some properties of the energy levels and wave functions of H_2O in the ground state first.

Before continuing our discussions, we note that usually states of the H_2O molecule are labelled by three quantum numbers j, k_a, and k_c. In the present study, sometimes we may use j and τ ($\equiv k_a - k_c$) to label a state because we want to use short labels, especially in figures. There is a simple way to recover the corresponding k_a and k_c values from j and τ. For the case where $j+\tau=2n$, $k_a=n$ and $k_c=j-n$. Meanwhile, for the case where $j+\tau=2n+1$, $k_a=n+1$ and $k_c=j-n$.

2.1. *Properties of energy levels*

With respect to the energy levels, we present rotational energy levels of H_2O with $j=11$ to 20 in the vibrational ground state provided by Barber *et al.* [10] versus j in Figure 1. In this plot energy levels of states with $j+k_a-k_c=$even are plotted by symbols $\times$ and those with $j+k_a-k_c=$odd are given by symbols Δ, respectively. In addition, for the former, their values of k_a-k_c are presented on the right side of $\times$ and for the latter, the values are on the left side of Δ. As shown in the figure, there are identities of the energy levels between pairs of the states with the same j. Thus, within certain small tolerances, the pair identity of the energy levels holds well. The higher the j is, the firmer the identity holds. With Figure 1, one can easily identify those paired states. They are pairs of two states with the same j and k_c ($=j-n$), but their $k_a=n$ or $n+1$ where $n=0,1,\ldots$ or two states with the same j and k_a ($=j-n$), but $k_c=n$ or $n+1$. We list some of them in braces: $\{j_{0,j},j_{1,j}\}$, $\{j_{1,j-1},j_{2,j-1}\}$, $\{j_{2,j-2},j_{3,j-2}\},\ldots,$ $\{j_{j-2,3},j_{j-2,2}\},\{j_{j-1,2},j_{j-1,1}\}$, and $\{j_{j,1},j_{j,0}\}$. Besides this pair identity feature, one can conclude that for each of these pairs, their energy levels vary smoothly as j varies and these variation patterns are well organized along the j axis.

2.2. *Properties of wave functions*

With respect to wave functions of the H_2O states, they are given in terms of expansion coefficients $U^j_{k\tau}$ over the symmetric top wave functions $|jkm\rangle$ with $k=-j$, $-j+1,\ldots,j$,

$$|j\tau m\rangle = \sum_k U^j_{k\tau}\,|jkm\rangle. \tag{1}$$

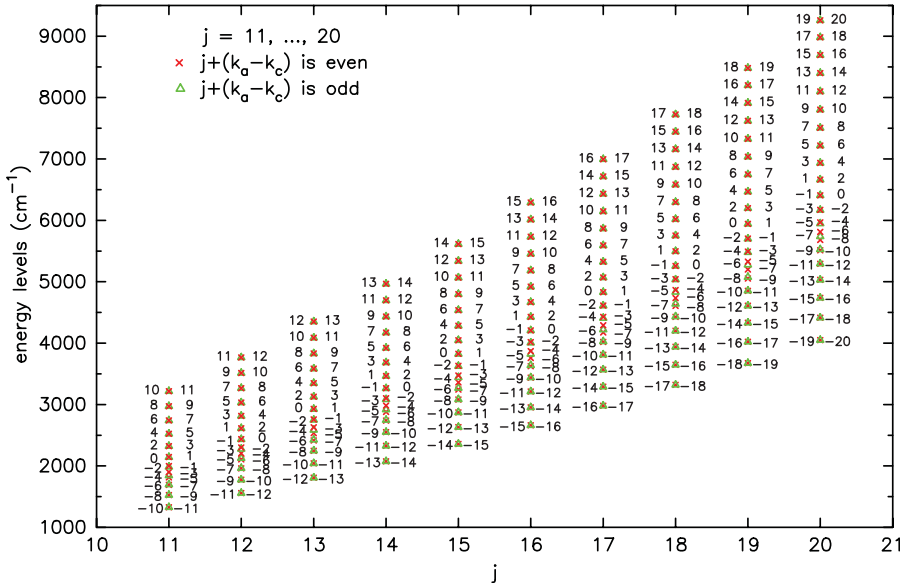

Figure 1. A plot to show energy levels of H_2O states with $j=11$ to 20 in the vibrational ground state [10]. For states with $j+k_a-k_c=$ even, their energy levels are plotted by × and their values of k_a-k_c are presented on the right side of the symbols. Meanwhile, for states with $j+k_a-k_c=$ odd, their energy levels are plotted by Δ and values of k_a-k_c are on the left side of the symbols.

Table 1. Symmetry classification by the parities of k_a and k_c.

	I R		I L		II R		II L		III R		III L	
	J_{even}	J_{odd}	J_{even}	J_{odd}	J_{even}	J_{odd}	J_{even}	J_{odd}	J_{even}	J_{odd}	J_{even}	J_{odd}
E^+	ee	eo	ee	eo	ee	oo	ee	oo	ee	oe	ee	oe
E^-	eo	ee	eo	ee	oo	ee	oo	ee	oe	ee	oe	ee
O^+	oo	oe	oe	oo	oe	eo	eo	oe	eo	oo	oo	eo
O^-	oe	oo	oo	oe	eo	oe	oe	eo	oo	eo	eo	oo

With the selected representation, states assigned either by the sub-block E^+ or by E^- have non-zero values of $U^j_{k\tau}$ only for k is even and states associated with O^+ or O^- have non-zero values only for k is odd. In addition, depending on the superscripts + and − in the sub-block symbols assigned, $U^j_{k\tau}$ is either an even function of k or an odd function of k. In the present study, we follow a convention adopted by Zare [9] to define the Wang functions and the symmetric top wave functions. With this convention, symmetry classification by the parities of k_a and k_c in the six representations is given by Table 1.

After outlining the basics about how to describe the wave functions, we exhibit their properties. First, we consider three sets of pairs of states $\{j_{j,0}, j_{j,1}\}$, $\{j_{j-1,1}, j_{j-1,2}\}$, and $\{j_{j-2,2}, j_{j-2,3}\}$and present their coefficients $U^j_{k\tau}$ starting from certain boundary values j_{bd} (i.e., 3, 5, and 7, respectively) to $j=26$ in corresponding Figures 2(a)–(c). For these states whose k_a are the maximum or close to the maximum, the I R representation is the best choice.

As shown in the figure, there are two striking features of these coefficients. First of all, coefficients of the paired states such as $j_{j,0}$ and $j_{j,1}$ with the same j are almost identical in the positive k axis and one becomes the other's mirror image in the negative k axis. In other words, their absolute values are always the same. It is worth mentioning that their opposite signs in the negative k axis are necessary to guarantee the orthogonality between their wave functions. Neglecting the sign difference in the negative k axis, we call this feature the pair identity of the wave functions. We note that the higher the j, the better the pair identity. Because the pair identity breaks down for $j<j_{bd}$, the plotting in Figure 2 starts from $j=j_{bd}$. Secondly, by comparing the coefficients associated with different

Downloaded by [NASA Goddard Institute for Space Studies] at 07:23 23 April 2013

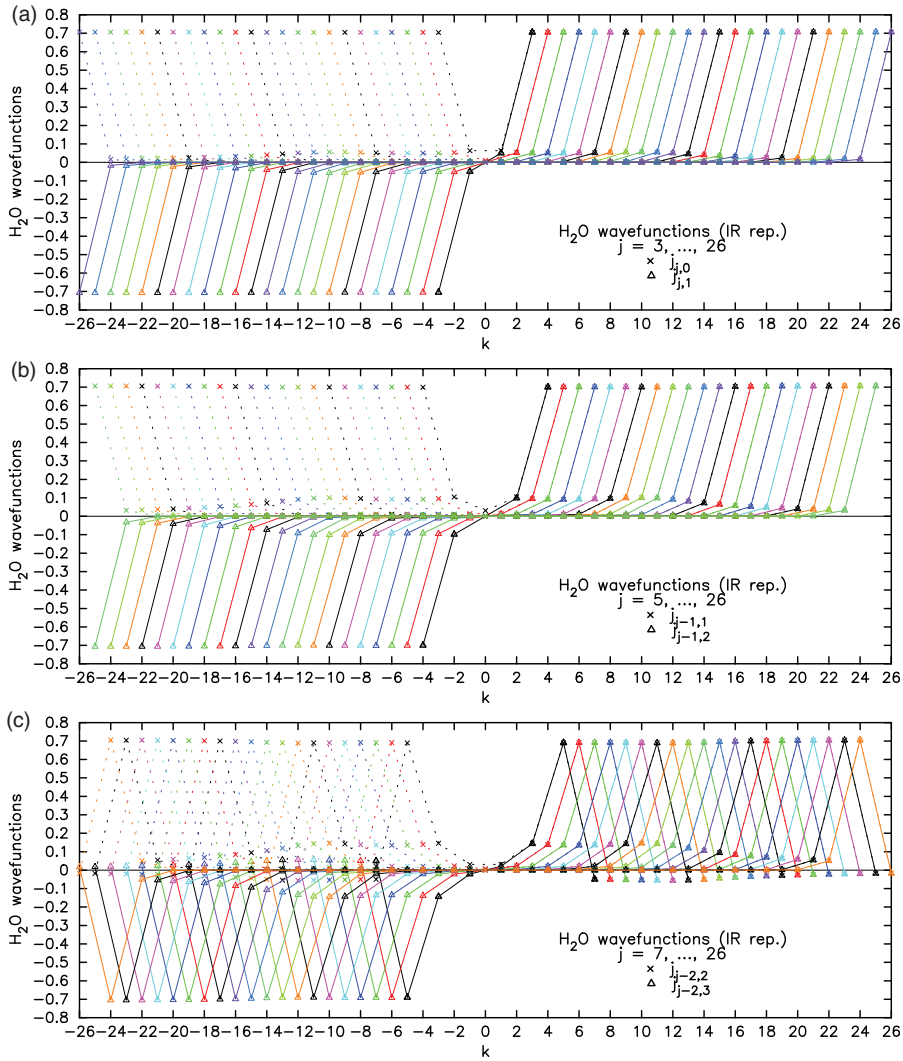

Figure 2. A plot to show properties of H_2O wave functions for three sets of pairs of states $\{j_{j,0}, j_{j,1}\}$, $\{j_{j-1,1}, j_{j-1,2}\}$, and $\{j_{j-2,2}, j_{j-2,3}\}$ for $j = j_{\mathrm{bd}}, \ldots, 26$. Their coefficients $U^j_{k\tau}$ with k ranging from $-j$ to j in the I R representation are represented by symbols $\times$ and Δ, respectively. Different colors are used to distinguish different j values and symbols associated with the same states are connected by dotted or solid lines.

j values, it is obvious that for members of the pairs such as $j_{j,0}$ with $j = 3, 4, \ldots,$ their patterns are very similar. As j varies, without any distortions, placements of the patterns shift horizontally along both the positive and negative k axes. We call this the pattern similarity of the wave functions. It is worthwhile emphasizing that these pattern similarities are valid only among members of these pairs. For example, they are valid within a set of the states $j_{j,0}$ and within a set of the states $j_{j,1}$, and so on. Finally, by comparing Figures 2(a)–(c), values of the boundary j_{bd} increase from 3 to 5 to 7, respectively. This implies that as k_a decreases from the maximum, the pair identity and the smooth variation break down at higher and higher j values.

Now, we consider states whose k_c values are the maximum or close to it. In these cases, the III R representation is more suitable to describe the properties of the wave functions. We present coefficients $U^j_{k\tau}$ for three sets of pairs of states $\{j_{0,j}, j_{1,j}\}$, $\{j_{1,j-1}, j_{2,j-1}\}$, and $\{j_{2,j-2}, j_{3,j-2}\}$ starting from certain boundary values j_{bd} (i.e., 7, 10, and 13, respectively) to $j = 26$ in Figure 3. As shown in the figure, the pair identities and the pattern similarities appearing in Figure 2 for the previous three sets of pairs clearly hold there also, but it is noticeable that their validity boundaries become higher than those associated with the previous three sets.

In practice, for sets of paired states, one can find boundary estimations from plots to show their wave

Downloaded by [NASA Goddard Institute for Space Studies] at 07:23 23 April 2013

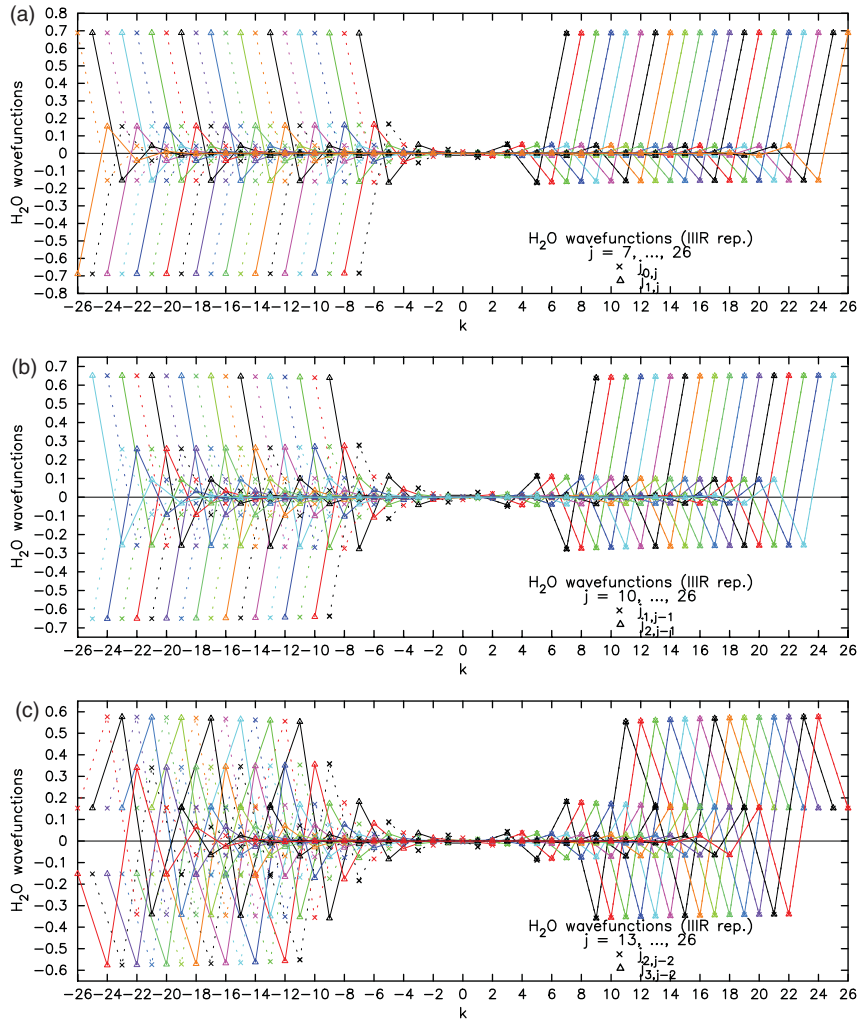

Figure 3. The same as Figure 2 except that the three sets of pairs of states are $\{j_{0,j}, j_{1,j}\}$, $\{j_{1,j-1}, j_{2,j-1}\}$, and $\{j_{2,j-2}, j_{3,j-2}\}$ and their wave functions are derived in the III R representation.

Table 2. Boundaries for different sets of paired H_2O states.

Set	$j_{j,0}$ $j_{j,1}$	$j_{j-1,1}$ $j_{j-1,2}$	$j_{j-2,2}$ $j_{j-2,3}$	$j_{j-3,3}$ $j_{j-3,4}$	$j_{j-4,4}$ $j_{j-4,5}$	$j_{j-5,5}$ $j_{j-5,6}$	$j_{j-6,6}$ $j_{j-6,7}$	...	$j_{4,j-4}$ $j_{5,j-4}$	$j_{3,j-3}$ $j_{4,j-3}$	$j_{2,j-2}$ $j_{3,j-2}$	$j_{1,j-1}$ $j_{2,j-1}$	$j_{0,j}$ $j_{1,j}$
j_{bd}	3	5	7	9	10	12	14		19	16	13	10	7
ε (%)	0.63	0.66	0.49	0.32	1.08	0.60	0.32		1.28	0.55	1.13	1.00	0.60

functions such as Figures 2 and 3. Alternatively, for a set of paired states j,τ_1 and j,τ_2, by defining the relative difference of their wave functions ε as

$$\varepsilon = \sum_k \left| |U^j_{k\tau_2}|^2 - |U^j_{k\tau_1}|^2 \right| \Big/ \sum_k |U^j_{k\tau_1}|^2, \qquad (2)$$

one can calculate how ε varies with j and determine a boundary for this set. We note that ε is a numerical measure of the identity of the paired wave functions. We provide our suggested j_{bd} and their corresponding values of ε in Table 2. As shown in the table, we have chosen ε about 1% to determine j_{bd} and the latter match those estimated from the figures well.

In summary, with respect to the H_2O energy levels, there are pair identities and well organized variations exhibited within each of the sets of paired states whose

Downloaded by [NASA Goddard Institute for Space Studies] at 07:23 23 April 2013

Downloaded by [NASA Goddard Institute for Space Studies] at 07:23 23 April 2013

j values are high. Meanwhile, for the wave functions, there are pair identities and pattern similarities within each of the same sets defined in analysing the energy levels. In general, sets with small differences between j and $|k_a - k_c|$ have lower boundaries j_{bd} and those with large differences have higher ones. On the other hand, except for the pair identities, other properties of the energy levels and wave functions have individual characters. For example, similar patterns of the wave functions appearing in one set differ significantly from those in other sets. Furthermore, as explained above, these properties disappear for states whose j values are below certain boundaries and the latter vary with the sets.

There are useful explanations about symmetry assignments of H_2O wave functions for paired states. Besides, there are quantities associated with the energy levels and the wave functions which are important in the present study because they determine couplings between H_2O states. Readers can find discussions of these in sections A-1 and A-2 of the Appendix.

Finally, we would like briefly to point out that it is not difficult to explain why the paired states with high j values have almost the same energy levels and the wave functions. It is well known that the Hamiltonian of the H_2O molecule associated with the quantum number j can be expressed by a sub-block form consisting of four sub-matrices, E^+, E^-, O^+, and O^-. As an example, we assume $j =$ even and consider the pairs of $j_{j,0}$ and $j_{j,1}$. According to Table A-1 in the Appendix and Figure 1, $j_{j,0}$ is an eigenvector of E^+ with the largest eigenvalue and $j_{j,1}$ is an eigenvector of E^- with the largest eigenvalue. Both of these E^+ and E^- are tridiagonal and they are almost identical except for adding additional first low and first column in E^+. In addition, in comparison with their diagonal elements, their off-diagonal elements are small. The higher the j is, the more identical are E^+ and E^-. It turns out that their largest eigenvectors and eigenvalues are their ones least affected by their differences. As a result, they bear the identity feature the most. For other cases, similar arguments are also applicable, but we do not pursue this here.

3. General formalism in calculating half-widths for H_2O lines

After discussing the properties of the energy levels, wave functions, we briefly outline the formalism used to calculate the half-widths and shifts of H_2O lines.

The main computational task for calculating the Lorentzian half-widths is the evaluations of matrix elements appearing in the perturbation expansion of the $\hat{S}$ matrix ($=S_{\mathrm{I}} \cdot S_{\mathrm{F}}^*$, where S_{I} and S_{F} are scattering matrices in Hilbert space). Usually, in practice, these evaluations are limited to the second-order of the expansion. Within the RB formalism that has been widely used for calculating Lorentzian spectral line half-widths and shifts for decades [11–14], the original expression for the half-width is given by

$$\gamma_{RB} = \frac{n_b}{2\pi c}\int_0^{+\infty} v f(v)\mathrm{d}v \int_0^{+\infty} 2\pi b\,\mathrm{d}b \times \left\langle 1 - \cos[S_1(b) + \mathrm{Im}S_2(b)]e^{-\mathrm{Re}S_2(b)}\right\rangle_{j_2}, \quad (3)$$

where n_b is the number density of the bath molecule, $f(v)$ is the Maxwell–Boltzmann distribution function, S_1 and S_2 are matrix elements in the Liouville space associated with the first- and second-orders of the perturbation expansion of the Liouville operator $\hat{S}$, and $\langle\ \rangle_{j_2}$ means an average over the quantum number j_2 of the N_2 molecule. However, we have found a subtle error in the RB formalism [15]. After remedying this derivation error, the correct expression for the half-width in the 'modified' RB formalism (MRB) becomes [15]

$$\gamma_{MRB} = \frac{n_b}{2\pi c}\int_0^{+\infty} v f(v)\mathrm{d}v \int_0^{+\infty} 2\pi b\,\mathrm{d}b \times \left\{1 - \cos[\langle S_1(b)\rangle_{j_2} + \mathrm{Im}\langle S_2(b)\rangle_{j_2}]e^{-\mathrm{Re}\langle S_2(b)\rangle_{j_2}}\right\}. \quad (4)$$

We note that the essential difference between these two expressions is that in Equation (3) the summation over j_2 is outside of the cumulant expansion while in contrast, in Equation (4) it is inside. It is worthwhile emphasizing that because the bath average is carried out in the line space, an average over j_2 has been included. Thus, by understanding that S_1(b) and S_2(b) are the bath averages associated with the first- and second-order expansions of the Liouville operator, one can supress all of these $\langle\ \rangle_{j_2}$ in Equation (4). For simplicity, we will omit the subscript MRB of γ.

In the present study, we consider lines in the H_2O pure rotational band. Then, by ignoring negligible contributions from $\mathrm{Im}S_2$(b), making an approximation to replace the integration over the velocity by the averaged velocity $\bar{v}(=\sqrt{8kT/\pi m})$ and changing the integration variable impact parameter b and the lower limit 0 to the distance of closest approach r_c along trajectories and $r_{c,\min}$, the minimum value of r_c corresponding to strictly head-on collisions, respectively, one can obtain a simplified expression for the half-width

$$\gamma = \frac{n_b\bar{v}}{2\pi c}\int_0^{+\infty} 2\pi b\left[1 - e^{-\mathrm{Re}S_2(b)}\right]\mathrm{d}b = \frac{n_b\bar{v}}{2\pi c}\int_{r_{c,\min}}^{+\infty} 2\pi b\left(\frac{\mathrm{d}b}{\mathrm{d}r_c}\right)\left[1 - e^{-\mathrm{Re}S_2(r_c)}\right]\mathrm{d}r_c. \quad (5)$$

Downloaded by [NASA Goddard Institute for Space Studies] at 07:23 23 April 2013

The value of $r_{c,\min}$ can be determined by an energy conservation equation

$$\frac{2V_{iso}(r_{c,\min})}{m\bar{v}^2} - 1 = 0. \tag{6}$$

Usually, people prefer to represent S_2 by three components labelled by $S_{2,outer,i}$, $S_{2,outer,f}$, and $S_{2,middle}$, respectively. In the present study, we follow the same custom. As an example, an expression for $S_{2,outer,i}$ where the subscript i is a simple notation for the initial state $j_i\ \tau_i$ is given by [4]

$$\begin{aligned} S_{2,outer,i} = {} & \frac{1}{\hbar^2(2j_i+1)} \\ & \times \sum_{j_2} \rho_{j_2} \sum_{j_i'\tau_i'} \sum_{j_2'} \sum_{(m)} \int_{-\infty}^{\infty} \mathrm{d}t \\ & \times \int_{-\infty}^{t} \mathrm{d}t' e^{i(\omega_{j_i\tau_i j_i'\tau_i'} + \omega_{j_2 j_2'})(t-t')} \\ & \times \left\langle j_i\tau_i m_i j_2 m_2 | V(\vec{R}(t)) | j_i'\tau_i' m_i' j_2' m_2' \right\rangle \\ & \times \left\langle j_i'\tau_i' m_i' j_2' m_2' | V(\vec{R}(t')) | j_i\tau_i m_i j_2 m_2 \right\rangle. \end{aligned} \tag{7}$$

In the above equation, ρ_{j_2} is the density matrix of the bath molecule, $\omega_{j_i\tau_i j_i'\tau_i'}$ is given by equation (A-1), $\omega_{j_2 j_2'} = [E^{(b)}(j_2) - E^{(b)}(j_2')]/\hbar$, and $|j_i\tau_i m_i\, j_2 m_2\rangle = |j_i\tau_i m_i\rangle \otimes |j_2 m_2\rangle$ where $|j_i\tau_i m_i\rangle$ and $|j_2 m_2\rangle$ are the basis of Hilbert space for the H_2O and N_2 molecules, respectively.

In order to overcome convergence problems existing in usual line-shape theories involving the site–site potential models, we have developed a new formalism based on the coordinate representation. We will not provide a detailed development of the new formalism, but interested readers can find its derivation in our previous work [4,16]. Here, we only present some of the important formulas. By introducing the correlation functions $F_{L_1K_1K_1'L_2}(t)$ and their Fourier transforms $H_{L_1K_1K_1'L_2}(\omega)$ defined by

$$H_{L_1K_1K_1'L_2}(\omega) = \frac{1}{\sqrt{2\pi}} \int_{-\infty}^{\infty} e^{i\omega t} F_{L_1K_1K_1'L_2}(t)\mathrm{d}t. \tag{8}$$

the expression for the real part of $S_{2,outer,i}$ can be obtained as

$$\begin{aligned} \mathrm{Re}S_{2,outer,i}(r_c) = {} & \sqrt{\frac{\pi}{2}} \sum_{L_1K_1K_1'L_2} \sum_{j_i'\tau_i'} (2j_i'+1) \\ & \times D(j_i\tau_i j_i'\tau_i'; L_1K_1) D(j_i\tau_i j_i'\tau_i'; L_1K_1') \\ & \times \sum_{j_2 j_2'} (2j_2+1)(2j_2'+1)\rho_{j_2} \\ & \times C^2(j_2\, j_2'\, L_2, 000) \\ & \times H_{L_1K_1K_1'L_2}(\omega_{j_i\tau_i j_i'\tau_i'} + \omega_{j_2 j_2'}). \end{aligned} \tag{9}$$

We note that because the correlation functions $F_{L_1K_1K_1'L_2}(t)$ are associated with a specified trajectory, $\mathrm{Re}S_{2,outer,i}$ is a function of r_c. For clarity, we have explicitly added the argument r_c for $\mathrm{Re}S_{2,outer,i}$ in Equation (9). An expression for $\mathrm{Re}S_{2,outer,f}(r_c)$ is the same as $\mathrm{Re}S_{2,outer,i}(r_c)$ given in Equation (9) except for a replacement of j_i, τ_i by j_f, τ_f. Meanwhile, an expression for $S_{2,middle}(r_c)$ is given by

$$\begin{aligned} S_{2,middle}(r_c) = \sqrt{2\pi} \sum_{L_1K_1K_1'L_2} & \{(-1)^{L_1}(2j_i+1)(2j_f+1) \\ & \times W(j_i j_f j_i j_f; 1L_1) \\ & \times D(j_i\tau_i j_i\tau_i; L_1K_1) D(j_f\tau_f j_f\tau_f; L_1K_1')\} \\ & \times \sum_{j_2 j_2'} (2j_2+1)(2j_2'+1)\rho_{j_2} \\ & \times C^2(j_2 j_2' L_2, 000) H_{L_1K_1K_1'L_2}(\omega_{j_2 j_2'}). \end{aligned} \tag{10}$$

We note that with our new formalism, the main tasks to calculate N_2-broadened half-widths for H_2O lines are evaluations of several dozens of the correlations $F_{L_1K_1K_1'L_2}(t)$ labeled by a set of numbers consisting of one tensor rank L_1 with two subsidiary indices K_1, K_1' related to H_2O and another tensor rank L_2 for N_2 [4]. Because N_2 is a diatomic molecule, L_2 must be even. Thus, the number of sets is determined by the upper limits of L_1 and L_2. If one chooses the II R representation to develop the H_2O wave functions where the two H atoms are symmetrically located in the molecular-fixed frame, values of K_1 and K_1' must also be even. Due to symmetries, some of the correlation functions are identical. For examples, the four correlations labeled by (2 2 2 0), (2 2−2 0), (2−2 2 0) and (2−2−2 0) are identical. One can conveniently express this symmetry by $F_{L_1|K_1||K_1'|L_2}(t)$. In addition, there is another exchange symmetry between K_1 and K_1' in the correlation functions. Thus, the number of the correlations required to be evaluated can be reduced significantly.

Finally, as shown in Equations (9) and (10), the expressions for $\mathrm{Re}S_{2,outer,i}(r_c)$, $\mathrm{Re}S_{2,outer,f}(r_c)$, and $S_{2,middle}(r_c)$ are given by summations of contributions from individual correlations. As a result, among all correlations how important the individual correlation is depends on how large its magnitude is. For a specified correlation, the asymptotic behaviour of its magnitude as $r_c \to \infty$ is well defined. In general, (1000), (1002), (2|2||2|0), and (2|2||2|2) have large magnitudes and at $r_c \to \infty$ they vary as r_c^m with $m = -14$, -8, -16, and -10, respectively. In the present study, we will focus our attention on these correlations.

Downloaded by [NASA Goddard Institute for Space Studies] at 07:23 23 April 2013

4. Theoretical tools in analyzing calculated half-widths

4.1. *Harmonic expansions appearing in $S_{2,\,outer,\,i}(r_c)$ and $S_{2,\,outer,\,i}(r_c)$*

In the process of deriving Equation (9) for $\mathrm{Re}S_{2,\,outer,\,i}(r_c)$ from Equation (7), there is an intermediate expression for $S_{2,\,outer,\,i}(r_c)$ such that

$$S_{2,outer,i}(r_c) = \sum_{L_1 K_1 K_1' L_2} \int_0^\infty \mathrm{d}t\, W^{(a)}_{L_1K_1K_1'}(t; j_i\tau_i) W^{(b)}_{L_2}(t) F_{L_1K_1K_1'L_2}(t), \tag{11}$$

where two functions are defined by

$$W^{(a)}_{L_1K_1K_1'}(t; j_i\tau_i) = \sum_{j_i'\tau_i'} (2j_i'+1) D(j_i\tau_i j_i'\tau_i'; L_1K_1) \times D(j_i\tau_i j_i'\tau_i'; L_1K_1') e^{i\omega_{j_i\tau_i j_i'\tau_i'} t}, \tag{12}$$

and

$$W^{(b)}_{L_2}(t) = \sum_{j_2 j_2'} (2j_2+1)(2j_2'+1)\rho_{j_2} \times C^2(j_2 j_2' L_2, 000) e^{i\omega_{j_2 j_2'} t}, \tag{13}$$

respectively. It is worth mentioning that the correlation functions $F_{L_1K_1K_1'L_2}(t)$ depend on the potential and trajectory models. In contrast, the functions $W^{(a)}_{L_1K_1K_1'}(t; j_i\tau_i)$ and $W^{(b)}_{L_2}(t)$ are independent of these. On the other hand, $F_{L_1K_1K_1'L_2}(t)$ and $W^{(b)}_{L_2}(t)$ are common for all lines. Meanwhile, the functions $W^{(a)}_{L_1K_1K_1'}(t; j\tau)$ associated with j_i and τ_i and their partners associated with j_f and τ_f are only factors depending on the line of interest. They contain all information necessary to distinguish different amounts of contributions to the half-width of individual lines from the correlations to be considered.

It turns out that in Equations (12) and (13), both $W^{(a)}_{L_1K_1K_1'}(t; j_i\tau_i)$ and $W^{(b)}_{L_2}(t)$ are given in terms of harmonic expansions. Although these two functions are not periodic, their forms are very similar to the usual Fourier series. Thus, we borrow the concept of the Fourier series here. For later convenience, we rewrite Equation (12) as

$$W^{(a)}_{L_1K_1K_1'}(t; j_i\tau_i) = \sum_\alpha A_\alpha(L_1K_1K_1'; j_i\tau_i) e^{i\omega_\alpha(j_i\tau_i)t}, \tag{14}$$

where the summation index α represents a selected combination of j_i' and τ_i' in Equation (12), $\omega_\alpha(j_i\tau_i)$ stands for $\omega_{j_i\tau_i j_i'\tau_i'}$, and $A_\alpha(L_1K_1K_1'; j_i\tau_i)$ is defined by

$$A_\alpha(L_1K_1K_1'; j_i\tau_i) = (2j_i'+1) D(j_i\tau_i j_i'\tau_i'; L_1K_1) D(j_i\tau_i j_i'\tau_i'; L_1K_1'). \tag{15}$$

As usual, the 'Fourier series' of $W^{(a)}_{L_1K_1K_1'}(t; j_i\tau_i)$ are given by a set of components consisting of two values of $\omega_\alpha(j_i\tau_i)$ and $A_\alpha(L_1K_1K_1'; j_i\tau_i)$. The total number of components equals how many choices of α, and in general, there are several dozens of components. Fortunately, as shown later, there are only a few strong ones because many components are very weak. With Equations (A-2) and (15), one can show that

$$\sum_\alpha A_\alpha(L_1K_1K_1'; j_i\tau_i) = (2L_1+1)\delta_{K_1K_1'}. \tag{16}$$

The summation of $A_\alpha(L_1K_1K_1'; j_i\tau_i)$ over all α equals to $2L_1+1$ if $K_1 = K_1'$ or equals to 0 if $K_1 \neq K_1'$. We note that the above discussion is also applicable for analysing $\mathrm{Re}S_{2,\,outer,\,f}(r_c)$ where the 'Fourier series' of $W^{(a)}_{L_1K_1K_1'}(t; j_f\tau_f)$ are introduced.

Similarly, we can rewrite Equation (13) as

$$W^{(b)}_{L_2}(t) = \sum_\beta B_\beta(L_2) e^{i\omega_\beta t}, \tag{17}$$

where the summation index β represents a selected pair of j_2 and j_2', ω_β stands for $\omega_{j_2 j_2'}$, and $B_\beta(L_2)$ is given by

$$B_\beta(L_2) = (2j_2+1)(2j_2'+1)\rho_{j_2} C^2(j_2 j_2' L_2, 000). \tag{18}$$

Meanwhile, it is easy to show that the total intensity of the 'Fourier series' of $W^{(b)}_{L_2}(t)$ is equal to $2L_2+1$. In contrast with $A_\alpha(L_1K_1K_1'; j_i\tau_i)$ which are independent of the temperature, the 'Fourier series' of $W^{(b)}_{L_2}(t)$ depends slightly on the temperature.

Furthermore, by combining Equation (14) and Equation (17), we have

$$\begin{aligned} W^{(a)}_{L_1K_1K_1'}(t; j_i\tau_i) W^{(b)}_{L_2}(t) &= \sum_\alpha \sum_\beta A_\alpha(L_1K_1K_1'; j_i\tau_i) B_\beta(L_2) e^{i[\omega_\alpha(j_i\tau_i)+\omega_\beta]t} \\ &= \sum_\gamma E_\gamma(L_1K_1K_1'L_2; j_i\tau_i) e^{i\omega_\gamma(j_i\tau_i)t}, \end{aligned} \tag{19}$$

where γ is a simple notation for a set of j_i', τ_i', j_2, j_2', $\omega_\gamma(j_i\tau_i) = \omega_{j_i\tau_i j_i'\tau_i'} + \omega_{j_2 j_2'}$, and $E_\gamma(L_1K_1K_1'L_2; j_i\tau_i) = A_\alpha(L_1K_1K_1'; j_i\tau_i) B_\beta(L_2)$. After having the expressions for $E_\gamma(L_1K_1K_1'L_2; j_i\tau_i)$ and $\omega_\gamma(j_i\tau_i)$ available and knowing all accessible choices of γ, one can simply rewrite $\mathrm{Re}S_{2,\,outer,\,i}(r_c)$ as

$$\mathrm{Re}S_{2,outer,i}(r_c) = \sqrt{\frac{\pi}{2}} \sum_{L_1K_1K_1'L_2} \sum_\gamma E_\gamma(L_1K_1K_1'L_2; j_i\tau_i) \times H_{L_1K_1K_1'L_2}[\omega_\gamma(j_i\tau_i)]. \tag{20}$$

This expression clearly shows for an H_2O line of interest, how contributions to the $\mathrm{Re}S_{2,\,outer,\,i}(r_c)$ term from individual correlations are calculated. First of all, one determines a set of pairs $E_\gamma(L_1K_1K_1'L_2; j_i\tau_i)$ and

$\omega_\gamma(j_i\tau_i)$ with all accessible choices of the γ. We note that in contrast with the correlations that are common for all H_2O lines and depend on the interaction and trajectory models, this set of pairs depends on the line of interest but is independent of the interaction and trajectory models. In the next step, for an individual correlation, one picks up values of its Fourier transform $H_{L_1K_1K_1'L_2}(\omega)$ at $\omega=\omega_\gamma(j_i\tau_i)$, multiplies the latter by the corresponding values of $E_\gamma(L_1K_1K_1'L_2;j_i\tau_i)$, and adds up all the results to obtain the total contributions from this correlation. One then repeats the above step for each of the correlations, and finally one adds up contributions from all correlations to obtain the final result.

4.2. *General properties of the 'Fourier series' of* $W^{(a)}_{L_1K_1K_1'}(t;j\tau)$

We outline some properties of $W^{(a)}_{L_1K_1K_1'}(t;j\tau)$ that are very helpful in calculating contributions to $\mathrm{Re}S_{2,\,outer,\,i}(r_c)$ and $\mathrm{Re}S_{2,\,outer,\,f}(r_c)$ from the correlations. For simplicity, as long as their arguments are not involved in discussions, $W^{(a)}_{L_1K_1K_1'}(t;j\tau)$ is simplified to $W^{(a)}_{L_1K_1K_1'}$. First of all, it is obvious that there is an exchange symmetry between K_1 and K_1' such that

$$W^{(a)}_{L_1K_1K_1'}=W^{(a)}_{L_1K_1'K_1}. \tag{21}$$

Secondly, based on the fact that there is a symmetry property for the product of $U^j_{k\tau}$ and $U^j_{k'\tau}$

$$U^j_{k\tau}U^j_{k'\tau}=U^j_{-k\tau}U^j_{-k'\tau} \tag{22}$$

that is valid no matter which sub-blocks (E^+, E^-, O^+, and O^-) the wave functions of H_2O states belong. With this symmetry property, one can show that

$$W^{(a)}_{L_1K_1K_1'}=W^{(a)}_{L_1-K_1-K_1'}. \tag{23}$$

As a result, we know that some of $W^{(a)}_{L_1K_1K_1'}$ with different K_1 and K_1' are identical. For example, $W^{(a)}_{222}=W^{(a)}_{2-2-2}$, $W^{(a)}_{220}=W^{(a)}_{202}=W^{(a)}_{2-20}=W^{(a)}_{20-2}$, and so on.

On the other hand, the four correlations (2 2 2 0), (2−2−2 0), (2 2−2 0) and (2−2 2 0) are identical and the other four correlations (2 2 2 2), (2−2−2 2), (2 2−2 2) and (2−2 2 2) are identical. Then, with Equation (11) one can conclude that contributions to $S_{2,\,outer,\,i}(r_c)$ and $S_{2,\,outer,\,f}(r_c)$ from the correlations (2 2 2 0) and (2−2−2 0) are the same because not only $W^{(a)}_{222}=W^{(a)}_{2-2-2}$, but also these two correlations are identical. Among the eight correlations listed above, similar conclusions are also true for the pair of (2 2 2 2) and (2−2−2 2), for (2 2−2 0) and (2−2 2 0), and for (2 2−2 2) and (2−2 2 2). There are many similar identities valid for other correlations. Based on these identity properties, one is able to significantly reduce CPU times required when performing numerical calculations for the half-widths of H_2O lines.

Besides, with Equation (16) one knows that a summation of $A_n(L_1K_1K_1';j_i\tau_i)$ over all n equals to $2L_1+1$ if $K_1=K_1'$ or equals to 0 if $K_1\neq K_1'$. For examples, the total intensity of the spectrum for $W^{(a)}_{222}$ is 5, meanwhile the summation of the Fourier series of $W^{(a)}_{22-2}$ is zero. For the latter, the summations over its positive coefficients and over its negative ones are equal to 2.5 and −2.5, respectively. This implies that when contributions to $S_{2,\,outer,\,i}(r_c)$ and $S_{2,\,outer,\,f}(r_c)$ from the correlations (22–20) are added up, significant cancelations would happen between the positive and negative coefficients associated with $W^{(a)}_{22-2}(t)$. As a result, the net contributions from (22–20) are dramatically reduced. Numerical results show that in comparison with (2220), the contributions from (22–20) are several times smaller. Given the fact that these two correlations are completely identical, it is the different properties of $W^{(a)}_{222}$ and $W^{(a)}_{2-22}$ that play crucial roles here in determining which one is dominant. With respect to other correlations, similar conclusions are also true. Based on these conclusions, one knows which correlations are important and which are not. This is helpful in our quantitative analyses.

4.3. *Spectra of* $W^{(a)}_{L_1K_1K_1'}(\omega;j\tau)$

In order to exploit the benefits of the 'Fourier series' of $W^{(a)}_{L_1K_1K_1'}(t;j\tau)$ and to exhibit their intrinsic properties, one examines how they vary with members within the sets of paired states defined previously in analyzing the energy levels and the wave functions. According to definitions of the sets, states belonging to the same sets are paired with their partners and each of the pairs is distinguished by one parameter (i.e., the quantum number j). Then, by applying the knowledge on the D matrices developed in Section A-2 of the Appendix, one can predict that there are identities between spectra associated with two paired states in the same sets, and one can also expect that these distribution patterns would vary smoothly as the pairs of interest vary.

We choose $W^{(a)}_{100}(t;j\tau)$ as an example. In calculating contributions to $\mathrm{Re}S_{2,\,outer,\,i}(r_c)$ or $\mathrm{Re}S_{2,\,outer,\,f}(r_c)$, these spectra are the most important ones because the correlations (1000) and (1002) associated with them are the largest among all the correlations. First of all, we consider the sets of two paired states $j_{j-n,\,n}$ and $j_{j-n,\,n+1}$ with $j=j_{\mathrm{bd}},\,j_{\mathrm{bd}}+1,\ldots$ where n could be one among $0,1,\ldots$. We are interested in comparing the 'Fourier series' of $W^{(a)}_{100}(t;j\tau_1)$ and $W^{(a)}_{100}(t;j\tau_2)$ where

Downloaded by [NASA Goddard Institute for Space Studies] at 07:23 23 April 2013

Downloaded by [NASA Goddard Institute for Space Studies] at 07:23 23 April 2013

$\tau_1 = j - 2n$ and $\tau_2 = j - 2n - 1$. The former is a two dimensional array constructed by $\omega_{j\tau_1 j'\tau'_1}$ and $A_{j'\tau'_1}(100; j\tau_1)$ with j' and τ'_1 (or j', k'_{a1}, and k'_{c1}) running over all allowed selections where the expression for $A_{j'\tau'_1}(100; j\tau_1)$ is given by

$$A_{j'\tau'_1}(100; j\tau_1) = (2j' + 1)[D(j_{j-n,n} j'_{k'_{a1}, k'_{c1}}; 10)]^2. \quad (24)$$

Meanwhile, the latter is an array constructed by $\omega_{j\tau_2 j'\tau'_2}$ and $A_{j'\tau'_2}(100; j\tau_2)$ with j' and τ'_2 over all allowed selections where $A_{j'\tau'_2}(100; j\tau_2)$ is given by

$$A_{j'\tau'_2}(100; j\tau_2) = (2j' + 1)[D(j_{j-n,n+1} j'_{k'_{a2}, k'_{c2}}; 10)]^2. \quad (25)$$

Because the two original states $j_{j-n,n}$ and $j_{j-n,n+1}$ differ from each other only by $k_c = n$ and $k_c = n+1$, their non-zero coupling partners determined by the selection rule must have the same j' and k'_a, but with different k'_c values differing by 1. For example, as one picks a subsidiary state $j'_{j'-n,n+1}$ with $j' = j+1$ from the allowed coupling list for the original state $j_{j-n,n}$, one can find its corresponding subsidiary one $j'_{j'-n,n}$ appearing in the allowed coupling list for the original state $j_{j-n,n+1}$. It is obvious that these two subsidiary states $j'_{j'-n,n+1}$ and $j'_{j'-n,n}$ are paired states. Thus, one can conclude that the two D matrices $D(j_{j-n,n} j'_{j'-n,n+1}; 10)$ and $D(j_{j-n,n+1} j'_{j'-n,n}; 10)$ which appear in Equations (24) and (25), respectively, are paired also. Besides, the energy difference between the original $j_{j-n,n}$ and its coupling $j'_{j'-n,n+1}$ approximately equals to the difference between the original $j_{j-n,n+1}$ and its coupling $j'_{j'-n,n}$. This implies that the 'Fourier series' of $W^{(a)}_{100}(t; j\tau)$ associated with $j_{j-n,n}$ and that associated with $j_{j-n,n+1}$ have one identical component. By extending this discussion to other allowed couplings in their lists, one can conclude that these two paired states almost share identical components. Similar discussions can be carried out for the sets of pairs states $j_{n,j-n}$ and $j_{n+1,j-n}$ with $n = 0, 1, \ldots$. In summary, one should expect that any pairs of the states whose j values are above j_{bd} should share identity 'Fourier series'.

Concerning the analysis of how the spectra would vary with pairs within the same sets, one has to rely on plotting calculated spectra. For better visualization, one can consider the 'Fourier series' of $W^{(a)}_{100}(t; j\tau)$ as spectra $W^{(a)}_{100}(\omega; j\tau)$ consisting of many components. Each of their components can be imaged as a harmonics with $\omega_\alpha(j\tau)$ and $A_\alpha(100; j\tau)$ as its frequency and intensity. We would like to note that the terms of the spectrum and intensity are used here in describing the 'Fourier series' of $W^{(a)}_{100}(t; j\tau)$. Readers should not confuse these with those in describing resonance transitions for the H_2O molecule.

In the following, we select several different sets of the pairs and calculate their spectra of $W^{(a)}_{100}(\omega; j\tau)$. In Figure 4(a–c), we present the spectra for three sets of $\{j_{j,0}, j_{j,1}\}$, $\{j_{j-1,1}, j_{j-1,2}\}$, and $\{j_{j-2,2}, j_{j-2,3}\}$ with $j = j_{\mathrm{bd}} \cdots 21$ whose k_a values are the maximum or closer to the maximum and whose wave functions are plotted in Figure 2. In the plots, only j values of the pairs are explicitly provided. Based on these j values and definitions of the symbols in the plots, one can easily determine to which of the states the spectra belong. As shown in Figure 4(a–c), there are three or four branches consisting of main components from different states. By comparing the spectra between two paired states, one can conclude that their spectra are almost identical because two symbols □ and × are always overlapped. The higher the j is, the more identical their spectra. In addition, by looking at structures of the branches one can find that their patterns are well organized. This reflects the fact that their spectra vary very smoothly as j varies. Finally, by comparing the plots associated with the different sets, one can conclude that different sets have different spectral distributions. It is worth reiterating that the above claims are valid only for those states whose j values are above certain boundaries j_{bd} and the latter depend on the sets of interest.

Similarly, in Figure 5(a–c) we present the spectral distributions for another three sets of pairs $\{j_{0,j}, j_{1,j}\}$, $\{j_{1,j-1}, j_{2,j-1}\}$, and $\{j_{2,j-2}, j_{3,j-2}\}$ whose k_c values are the maximum or close to it and whose wave functions are plotted in Figure 3. We don't repeat the discussion and conclusions here because they are the same as those for the previous three sets. In summary, there are spectrum pair identities and spectrum pattern similarities within the sets defined previously.

There are several others of $W^{(a)}_{L_1 K_1 K'_1}(\omega; j\tau)$ with different choices of L_1, K_1, and K'_1. We expect that they could differ from each other dramatically. For example, the spectra of $W^{(a)}_{22-2}(\omega; j\tau)$ contain components with either positive or negative intensities such that its total intensity is zero. However, we believe that the pair identity and smooth variation features in describing $W^{(a)}_{100}(\omega; j\tau)$ within the same sets should remain valid for them also because these features result from the same sources: the properties of the energy levels and the wave functions.

4.4. *The 'Fourier series' of $W^{(b)}_{L_2}(t)$*

We now present profiles of the 'Fourier series' of $W^{(b)}_{L_2}(t)$ with $L_2 = 0, 2, \ldots$ which are common for all H_2O lines. It is obvious that the 'Fourier series' of $W^{(b)}_0(t)$ consists of only one term with its magnitude equals to 1 and $\omega = 0$. Next, we consider the 'Fourier series' of $W^{(b)}_2(t)$ which is the most important one among all $W^{(b)}_{L_2}(t)$ and

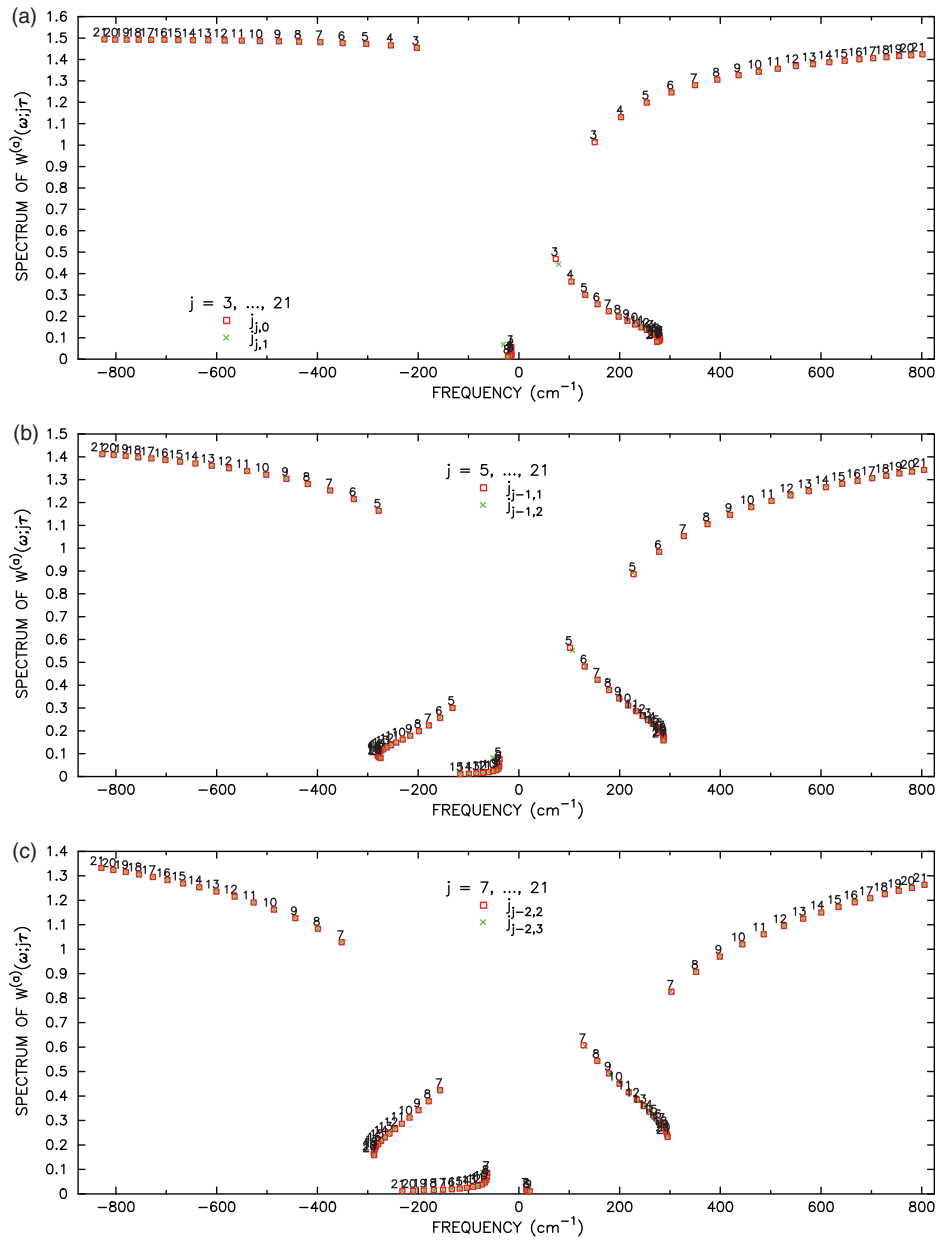

Figure 4. The spectra $W^{(a)}_{100}(\omega; j\tau)$ of three sets of the paired states $\{j_{j,0}, j_{j,1}\}$, $\{j_{j-1,1}, j_{j-1,2}\}$, and $\{j_{j-2,2}, j_{j-2,3}\}$ with $j = j_{\mathrm{bd}}, \ldots, 21$ whose k_a values are the maxima or closer to the maxima. For each of the pairs, spectra of the two paired states are plotted by symbols of □ and × in (a) – (c), respectively. Meanwhile, their j values are printed above the symbols □.

present its spectrum at $T = 296$ K in Figure 6. As shown in the figure, the spectra consists of many components, but the one located at $\omega = 0$ is overwhelmingly larger than the others.

4.5. *Samples of the 'Fourier series' of* $W^{(a)}_{L_1K_1K'_1}(t; j\tau)\, W^{(b)}_{L_2}(t)$

We now consider spectra associated with the 'Fourier series' of $W^{(a)}_{L_1K_1K'_1}(t; j\tau)\, W^{(b)}_{L_2}(t)$. We note that although $W^{(a)}_{L_1K_1K'_1}(t; j\tau)$ are independent of the temperature, but $W^{(b)}_2(t)$ depends on the temperature slightly. As a result, the 'Fourier series' of $W^{(a)}_{L_1K_1K'_1}(t; j\tau)\, W^{(b)}_{L_2}(t)$ would vary slightly with T also.

First of all, it is obvious that the spectra associated with $W^{(a)}_{L_1K_1K'_1}(t; j\tau) W^{(b)}_0(t)$ are the same as that of $W^{(a)}_{L_1K_1K'_1}(\omega; j\tau)$ because the spectrum associated with $W^{(b)}_0(t)$ consists of only one component located at $\omega = 0$ with a unit intensity. With respect to the spectra for $W^{(a)}_{L_1K_1K'_1}(t; j\tau) W^{(b)}_2(t)$, one expects their main patterns

Downloaded by [NASA Goddard Institute for Space Studies] at 07:23 23 April 2013

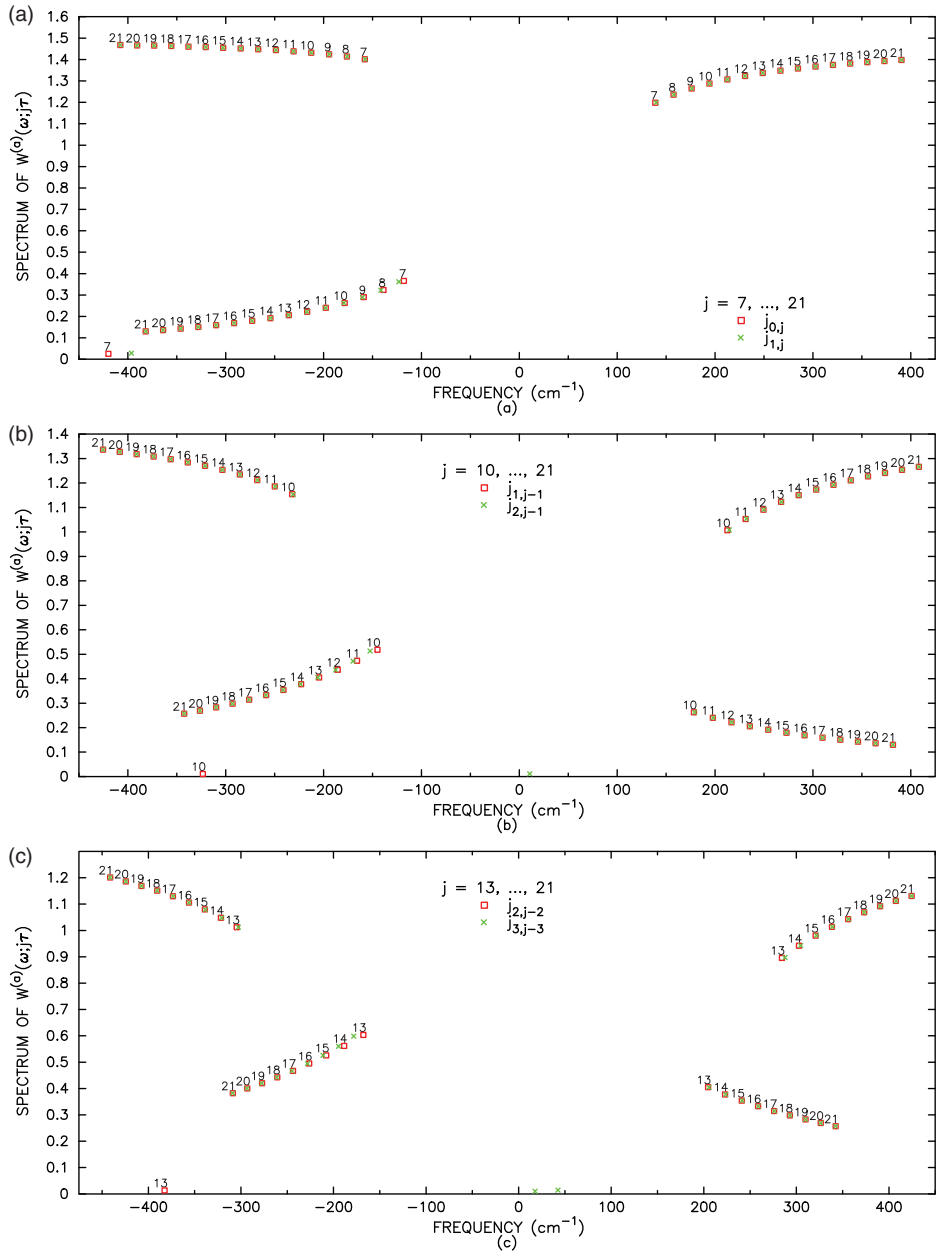

Figure 5. The same as Figure 4 except for three sets of pairs $\{j_{0,j}, j_{1,j}\}$, $\{j_{1,j-1}, j_{2,j-1}\}$, and $\{j_{2,j-2}, j_{3,j-2}\}$ whose k_c values are the maxima or closer to the maxima.

are similar to that of $W^{(a)}_{L_1K_1K_1'}(\omega; j\tau)$ because the dominant component of $W^{(b)}_2(\omega)$ is located at $\omega = 0$ and its other components are weak.

In order to demonstrate this claim more clearly, we present the spectra of $W^{(a)}_{100}(\omega; j\tau)$ for two paired states $10_{0,10}$ and $10_{1,10}$ in Figure 7. As shown by the figure, their spectra contain two major components accounting for 90.7% of the total intensity and one minor one. Then, we present the spectra of the 'Fourier series' $W^{(a)}_{100}(t; j\tau)W^{(b)}_2(t)$ for them in Figure 8. By comparing Figures 7 and 8, it is clear that the whole spectra share the main features of $W^{(a)}_{100}(\omega; j\tau)$, but have more small structures due to co-adding many weak components in $W^{(b)}_2(\omega)$.

In the present study, we want to investigate why and how the calculated half-widths vary with lines of interest. Because the Fourier transforms $H_{L_1K_1K_1'L_2}(\omega)$ are common for all lines, the 'Fourier series' of $W^{(a)}_{L_1K_1K_1'}(t; j\tau)W^{(b)}_{L_2}(t)$ contain all the information necessary to distinguish contributions to $\mathrm{Re}S_{2,\,outer,\,i}\,(r_c)$ and $\mathrm{Re}S_{2,\,outer,\,f}\,(r_c)$ for different H_2O lines. Given the fact that the spectra of $W^{(b)}_{L_2}(\omega)$ are independent of lines,

Downloaded by [NASA Goddard Institute for Space Studies] at 07:23 23 April 2013

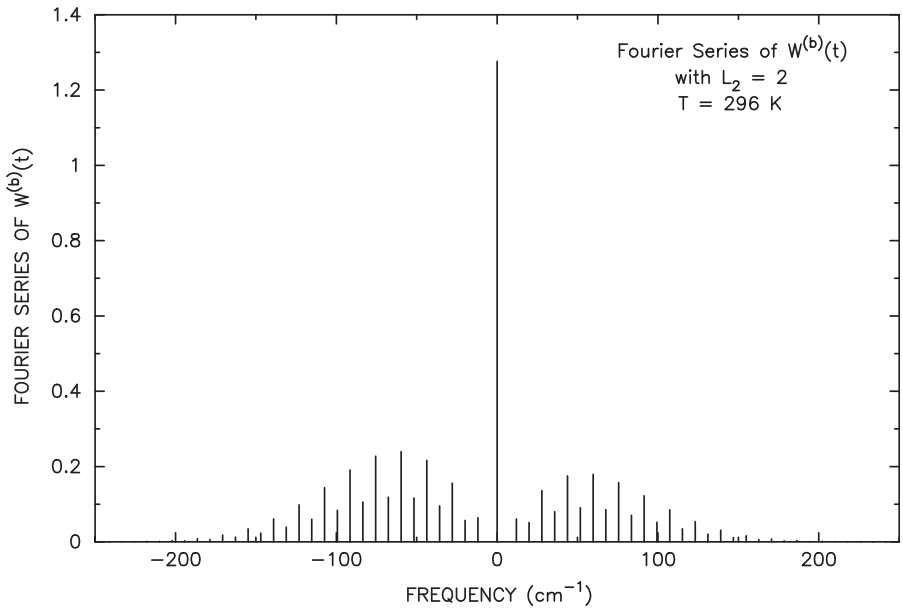

Figure 6. The 'Fourier series' of $W_2^{(b)}(t)$ with $L_2 = 2$ at $T = 296$ for the bath molecule N_2.

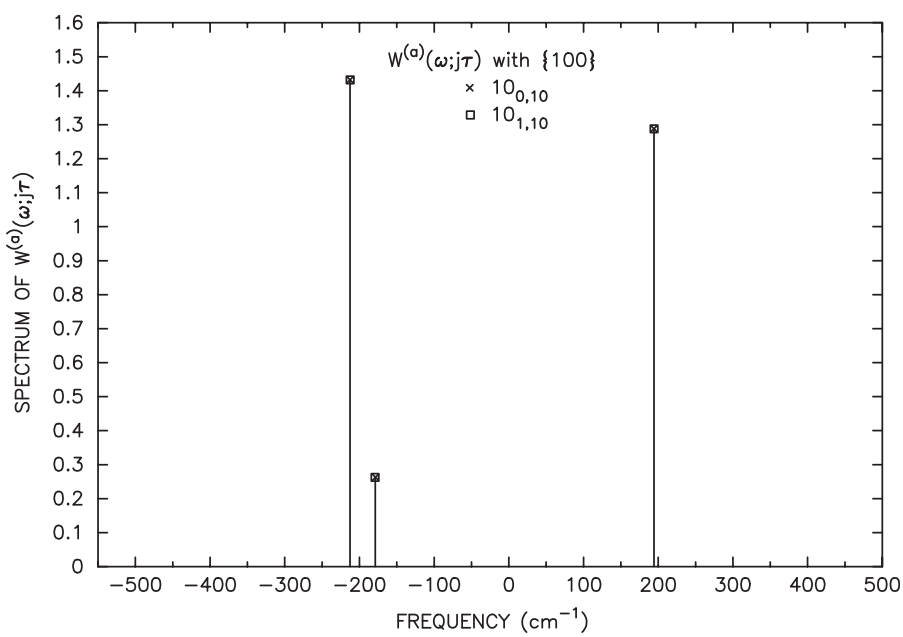

Figure 7. The spectra of $W_{100}^{(a)}(\omega\,; j\tau)$ for two paired states $10_{0,10}$ and $10_{1,10}$. The former is given by × and the latter by □.

the only factor to distinguish contributions for individual lines of $j_f\ \tau_f \leftarrow j_i\ \tau_i$ are their spectra of $W^{(a)}_{L_1K_1K_1'}(\omega; j_i\tau_i)$ and $W^{(a)}_{L_1K_1K_1'}(\omega; j_f\tau_f)$. In addition, we have shown these spectra represent main features of the whole spectra well. Thus, we believe all results and conclusions obtained from analysing $W^{(a)}_{L_1K_1K_1'}(\omega; j\tau)$ are similar to those that would be derived if the entire spectra were taken into account. Thus, in the following analyses we only focus on the spectra of $W^{(a)}_{L_1K_1K_1'}(\omega; j\tau)$.

Alternatively, one can argue that among all possible choices of $\omega_{j_2j_2'}$, many of them are zero. For those remaining, one can assume $|\omega_{j_2j_2'}| \ll |\omega_{j\tau j'\tau'}|$ because the rotational constant of the N_2 molecule is small.

Downloaded by [NASA Goddard Institute for Space Studies] at 07:23 23 April 2013

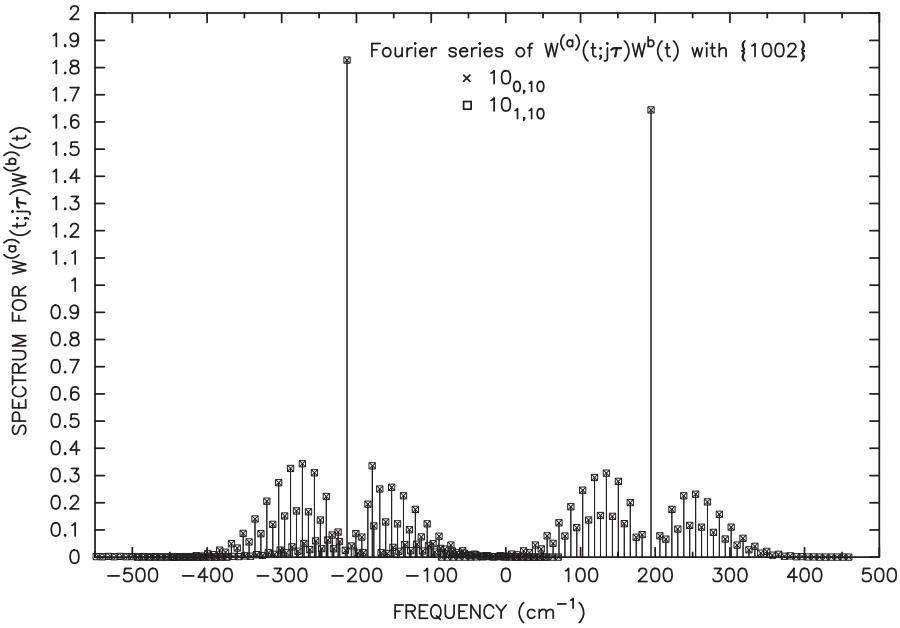

Figure 8. The spectra of the 'Fourier series' of $W^{(a)}_{100}(t\,;j\tau)\,W^{(b)}_{2}(t)$ at $T=296$ K for two paired states $10_{0,10}$, and $10_{1,10}$. They are given by × and □, respectively.

Then, by approximating $\omega_\mu(j\tau)$ $(=\omega_{j\tau j'\tau'}+\omega_{j_2 j_2'})$ by $\omega_\alpha(j\tau)$ $(=\omega_{j\tau j'\tau'})$, Equation (20) can be simplified

$$\begin{aligned}&\mathrm{Re}S_{2,outer,i}(r_c)\\&\approx\sqrt{\frac{\pi}{2}}\sum_{L_1K_1K_1'L_2}(2L_2+1)\\&\quad\times\sum_{\alpha}A_\alpha(L_1K_1K_1';j_i\tau_i)H_{L_1K_1K_1'L_2}[\omega_\alpha(j_i\tau_i)].\end{aligned}\tag{26}$$

Therefore, we have demonstrated that one can use the simpler spectra $W^{(a)}_{L_1K_1K_1'}(\omega;j\tau)$ to analyze contributions to $\mathrm{Re}S_{2,\,outer,\,i}(r_c)$ and $\mathrm{Re}S_{2,\,outer,\,f}(r_c)$. In comparison with Equation (20), the number of choices for the α in Equation (26) is much smaller than that for the γ.

4.6. *The term of $S_{2,\,middle}(r_c)$*

With respect to $S_{2,\,middle}(r_c)$, it can be expressed as

$$\begin{aligned}S_{2,middle}(r_c)&=\sum_{L_1K_1K_1'L_2}P_{L_1K_1K_1'}(j_f\tau_fj_i\tau_i)\\&\quad\times\int_{-\infty}^{\infty}\mathrm{d}tW^{(b)}_{L_2}(t)F_{L_1K_1K_1'L_2}(t)\\&=\sqrt{2\pi}\sum_{L_1K_1K_1'L_2}P_{L_1K_1K_1'}(j_f\tau_fj_i\tau_i)B_{L_1K_1K_1'L_2}(r_c).\end{aligned}\tag{27}$$

In the above expression, $P_{L_1K_1K_1'}(j_f\tau_fj_i\tau_i)$ and $B_{L_1K_1K_1'L_2}(r_c)$ are defined by

$$\begin{aligned}&P_{L_1K_1K_1'}(j_f\tau_fj_i\tau_i)\\&\quad=(-1)^{L_1}(2j_i+1)(2j_f+1)W(j_ij_fj_ij_f;1L_1)\\&\qquad\times D(j_i\tau_ij_i\tau_i;L_1K_1)D(j_f\tau_fj_f\tau_f;L_1K_1'),\end{aligned}\tag{28}$$

and

$$\begin{aligned}B_{L_1K_1K_1'L_2}(r_c)&=\sum_{j_2j_2'}(2j_2+1)(2j_2'+1)\rho_{j_2}\\&\quad\times C^2(j_2j_2'L_2,000)H_{L_1K_1K_1'L_2}(\omega_{j_2j_2'})\\&=\sum_{\beta}B_\beta(L_2)H_{L_1K_1K_1'L_2}(\omega_\beta),\end{aligned}\tag{29}$$

respectively. In comparison with the expressions for $\mathrm{Re}S_{2,\,outer,\,i}(r_c)$ in Equation (20), the expression for $S_{2,\,middle}(r_c)$ in Equation (27) is simpler because it is a product of two factors which are not interwoven. The factor of $B_{L_1K_1K_1'L_2}(r_c)$ is a function of r_c and it is common for all lines. In contrast, the factor of $P_{L_1K_1K_1'}(j_f\tau_fj_i\tau_i)$ is a constant and its value depends on the line of interest. Thus, with respect to a specified correlation, how its contributions to $S_{2,\,middle}(r_c)$ would vary as r_c varies depends only on $B_{L_1K_1K_1'L_2}(r_c)$, and meanwhile the magnitude for the line $j_f\,\tau_f\leftarrow j_i\,\tau_i$ would be proportional to the value of $F_{L_1K_1K_1'}(j_f\tau_fj_i\tau_i)$.

As mentioned previously, similar to $\mathrm{Re}S_{2,\,outer,\,i}(r_c)$ and $\mathrm{Re}S_{2,\,outer,\,f}(r_c)$, contributions to $S_{2,\,middle}(r_c)$ from individual correlations are also additive. It is not

Downloaded by [NASA Goddard Institute for Space Studies] at 07:23 23 April 2013

difficult to show there are no contributions to $S_{2,\,middle}(r_c)$ from correlations with odd L_1 because the matrix elements $D(j\tau j\tau; LK)$ are zero. In fact, with Equation (22) one can show that

$$D(j\tau j\tau; LK) = (-1)^{L+K} D(j\tau j\tau; LK). \tag{30}$$

Because we use the II R representation to describe the wave functions of H_2O, the indices K_1 and K_1' of the correlations must be even. As a result, Equation (30) means that $D(j\tau j\tau; LK)$ are zero unless L is even. Therefore, we know that there are no contributions to $S_{2,\,middle}(r_c)$ from all the correlations with odd L_1 values.

At this stage we would like to discuss the symmetries associated with $P_{L_1K_1K_1'}(j_f\tau_f j_i\tau_i)$ and $B_{L_1K_1K_1'L_2}(r_c)$. First of all, with Equation (22) one can also show that

$$D(j\tau j\tau; L-K) = D(j\tau j\tau; LK). \tag{31}$$

Based on this one can conclude that, as long as $|K_1|$ remains the same, the values of $P_{L_1K_1K_1'}(j_f\tau_f j_i\tau_i)$ associated with different K_1 are identical. The same conclusion is also true for K_1'. One can conveniently express this symmetry as $P_{L_1|K_1||K_1'|}(j_f\tau_f j_i\tau_i)$. However, there is no exchange symmetry between K_1 and K_1' in $P_{L_1K_1K_1'}(j_f\tau_f j_i\tau_i)$.

Secondly, we discuss symmetry properties of $B_{L_1K_1K_1'L_2}(r_c)$. With Equation (29), one can conclude that symmetries of $B_{L_1K_1K_1'L_2}(r_c)$ are determined by $H_{L_1K_1K_1'L_2}(\omega_m)$ and the latter's are the same as those of the correlation function. Therefore, we know that $B_{2220}(r_c) = B_{2-2-20}(r_c) = B_{22-20}(r_c) = B_{2-220}(r_c)$ and $B_{2222}(r_c) = B_{2-2-22}(r_c) = B_{22-22}(r_c) = B_{2-222}(r_c)$. Similarly, one can express this symmetry as $B_{L_1|K_1||K_1'|L_2}(r_c)$. In addition, there is an exchange symmetry between K_1 and K_1' in $B_{L_1K_1K_1'L_2}(r_c)$.

Finally, it is worth mentioning here that with respect to making contributions to $S_{2,\,middle}(r_c)$, correlations with $K_1 \neq K_1'$ and $K_1 = K_1'$ are comparable. This contrasts with $S_{2,\,outer,\,i}(r_c)$ and $S_{2,\,outer,\,f}(r_c)$ where correlations with $K_1 \neq K_1'$ are much less important than those with $K_1 = K_1'$. As a result, in comparison with $S_{2,\,outer,\,i}(r_c)$ and $S_{2,\,outer,\,f}(r_c)$, how important $S_{2,\,middle}(r_c)$ is would depends on whether $K_1 = K_1'$ or $K_1 \neq K_1'$ for the correlation to be considered. In general, $S_{2,\,outer,\,i}(r_c)$ and $S_{2,\,outer,\,f}(r_c)$ are larger than $S_{2,\,middle}(r_c)$, but this may not be true for correlations with $K_1 \neq K_1'$.

4.7. *Simplification in evaluating $S_{2,\,middle}(r_c)$*

It turns out that among all $B_{L_1K_1K_1'L_2}(r_c)$, the most important ones are $B_{2220}(r_c)$ and $B_{2222}(r_c)$. Then, one can adopt a simpler approximate formula to calculate $S_{2,\,middle}(r_c)$

$$S_{2,middle}(r_c) = 4\sqrt{2\pi}P_{222}(j_i\tau_i j_f\tau_f)[B_{2220}(r_c) + B_{2222}(r_c)], \tag{32}$$

where the factor of 4 appearing on the right side of Equation (32) results from the four identical contributions for each $B_{2220}(r_c)$ and $B_{2222}(r_c)$. From Equation (32) one can draw two important conclusions about $S_{2,\,middle}(r_c)$. First, the pattern of $S_{2,\,middle}(r_c)$ (i.e., as a function of r_c as it varies) is mainly determined by $B_{2220}(r_c) + B_{2222}(r_c)$. Second, for specified H_2O lines their contributions to $S_{2,\,middle}(r_c)$ are roughly proportional to values of $F_{222}(j_f\tau_f j_i\tau_i)$. Thus, with these values, one is able to easily judge which lines would have large magnitudes of $S_{2,\,middle}(r_c)$ and which lines would have small ones. Therefore, values of $F_{222}(j_f\tau_f j_i\tau_i)$ play a crucial role to distinguish $S_{2,\,middle}(r_c)$ for different lines.

Based on the potential model used in updating HITRAN 2008 [17], the 20th order cut-off and the 'exact' trajectory model, we have derived the function of $4\sqrt{2\pi}[B_{2220}(r_c) + B_{2222}(r_c)]$ at T = 220, 296, and 340 K and present results in Figure 9. As shown in the figure, values of $4\sqrt{2\pi}[B_{2220}(r_c) + B_{2222}(r_c)]$ decrease as r_c increases from the starting point $r_{c,\min}$. Meanwhile, by comparing its magnitudes at different temperatures, one can conclude that the magnitudes slightly decrease as T increases.

On the other hand, one can easily evaluate values of $P_{222}(j_f\tau_f j_i\tau_i)$ for all H_2O lines of the pure rotational band listed in HITRAN from Equation (28). In contrast with $4\sqrt{2\pi}[B_{2220}(r_c) + B_{2222}(r_c)]$, $P_{222}(j_f\tau_f j_i\tau_i)$ is a constant, it does not depend on the temperature, and its values are independent of the potential and trajectory models used in calculations. When values of $P_{222}(j_f\tau_f j_i\tau_i)$ for all H_2O lines are available, it becomes very easy to obtain the corresponding $S_{2,\,middle}(r_c)$ terms approximately for individual lines of interest because one only needs to multiply $4\sqrt{2\pi}[B_{2220}(r_c) + B_{2222}(r_c)]$ by their $P_{222}(j_f\tau_f j_i\tau_i)$ values.

In order to exhibit intrinsic properties of $P_{222}(j_f\tau_f j_i\tau_i)$, one needs to calculate values for lines belonging to the individually defined groups. In Section 5, we will provide their definitions in detail. At present, we only note that each of the groups consists of a set of paired lines in a specified branch. As an example, we choose three groups, $\{j_{f0,j_f} \leftarrow j_{i1,j_i}, j_{f1,j_f} \leftarrow j_{i0,j_i}\}$, $\{j_{f1,j_f-1} \leftarrow j_{i2,j_i-1}, j_{f2,j_f-1} \leftarrow j_{i1,j_i-1}\}$, and $\{j_{f3,j_f-3} \leftarrow j_{i2,j_i-1}, j_{f4,j_f-3} \leftarrow j_{i1,j_i-1}\}$ in the R branch of the pure rotational band and present their calculated values in Figure 10. As shown in the figure, for two paired lines whose j values are not less than either of

Downloaded by [NASA Goddard Institute for Space Studies] at 07:23 23 April 2013

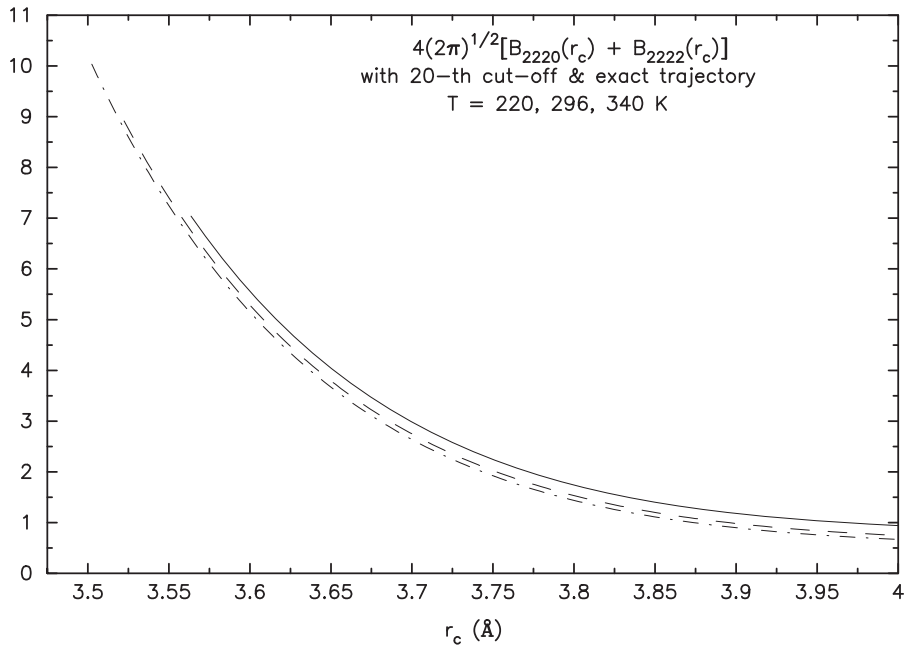

Figure 9. A plot to show profiles of $4\sqrt{2\pi}\ [B_{2220}(r_c) + B_{2222}(r_c)]$ at $T = 220$, 296, and 340 K. They are plotted by solid, dashed, and dash-dotted curves, respectively.

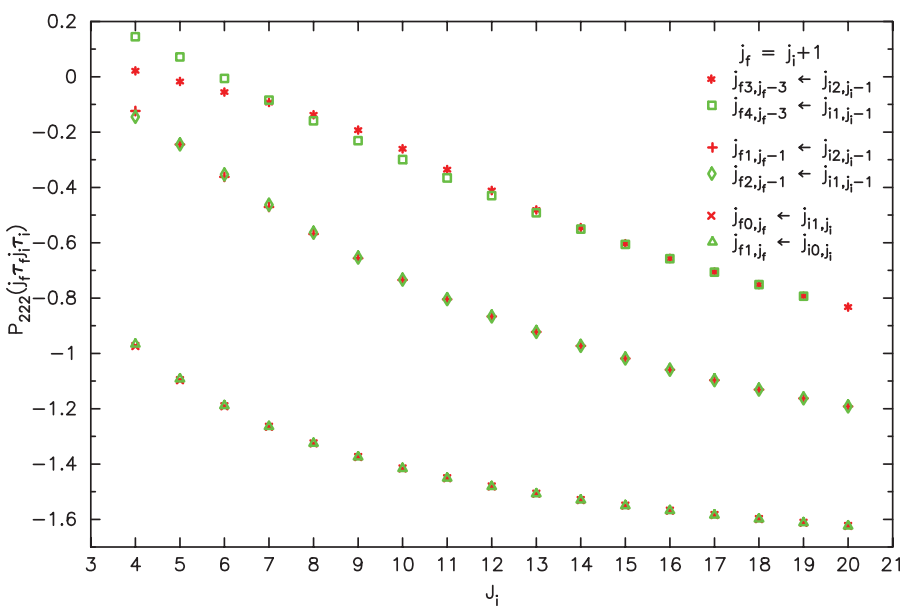

Figure 10. Calculated values of $P_{222}(j_f\tau_f j_i\tau_i)$ for three groups of H_2O lines $\{j_{f0,j_f} \leftarrow j_{i1,j_i}, j_{f1,j_f} \leftarrow j_{i0,j_i}\}$, $\{j_{f1,j_f-1} \leftarrow j_{i2,j_i-1}, j_{f2,j_f-1} \leftarrow j_{i1,j_i-1}\}$, and $\{j_{f3,j_f-3} \leftarrow j_{i2,j_i-1}, j_{f4,j_f-3} \leftarrow j_{i1,j_i-1}\}$ in the R branch listed in the pure rotational band of HITRAN. They are plotted by three pairs of symbols $\{\times, \Delta\}$, $\{+, \Diamond\}$, and $\{*, \Box\}$, respectively.

the j_{bd} associated with their initial and final states, their $P_{222}(j_f\tau_f j_i\tau_i)$ values are always identical. More specifically, for these three groups, as long as their members' j_i values are above 7, 10, and 15, respectively, their paired lines have identical $P_{222}(j_f\tau_f j_i\tau_i)$ values. Meanwhile, by looking at how their values vary as the pair of interest varies within the same groups, one can conclude that the variations with j_i are very smooth. Finally, by comparing values of $P_{222}(j_f\tau_f j_i\tau_i)$ with the same j_i among different

Downloaded by [NASA Goddard Institute for Space Studies] at 07:23 23 April 2013

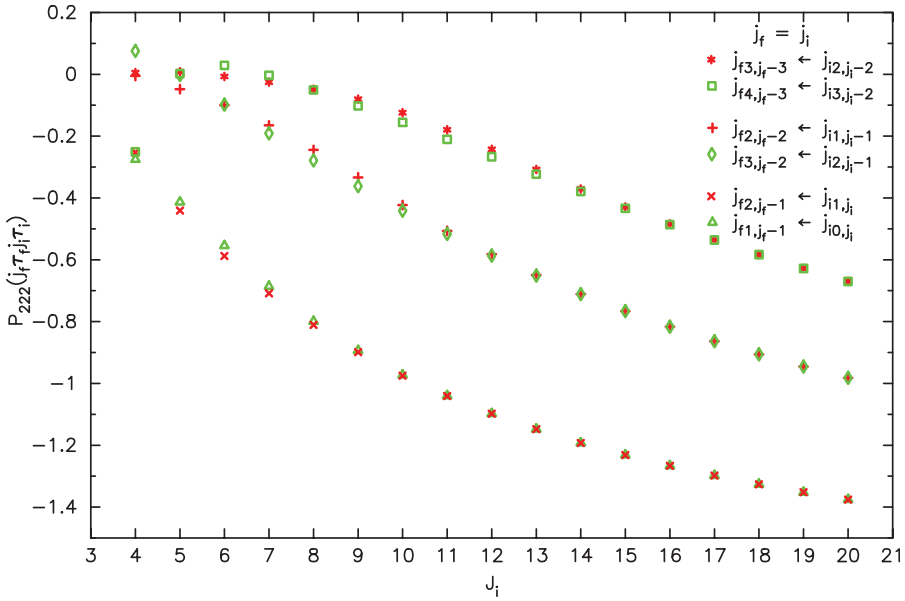

Figure 11. The same as Figure 10 except for three groups $\{j_{f2,j_f-1} \leftarrow j_{i1,j_i}, j_{f1,j_f-1} \leftarrow j_{i0,j_i}\}$, $\{j_{f2,j_f-2} \leftarrow j_{i1,j_i-1}, j_{f3,j_f-2} \leftarrow j_{i2,j_i-1}\}$, and $\{j_{f3,j_f-3} \leftarrow j_{i2,j_i-2}, j_{f4,j_f-3} \leftarrow j_{i3,j_i-2}\}$ in the Q branch.

groups, one can conclude the values could change dramatically.

As another example, we present results of $P_{222}(j_f\tau_f j_i\tau_i)$ for three groups $\{j_{f2,j_f-1} \leftarrow j_{i1,j_i}, j_{f1,j_f-1} \leftarrow j_{i0,j_i}\}$, $\{j_{f2,j_f-2} \leftarrow j_{i1,j_i-1}, j_{f3,j_f-2} \leftarrow j_{i2,j_i-1}\}$, and $\{j_{f3,j_f-3} \leftarrow j_{i2,j_i-2}, j_{f4,j_f-3} \leftarrow j_{i3,j_i-2}\}$ in the Q branch in Figure 11. We don't repeat the discussion here because the main conclusions are the same as above. We only note that for paired lines in these three groups, the pair identity of $P_{222}(j_f\tau_f j_i\tau_i)$ is valid starting from $j_i = 10$, 13, and 16, respectively.

5. Categorizations of H_2O lines and profiles of $\mathrm{Re}S_2(r_c)$ for lines within the same groups

We have shown that by dividing H_2O states into the sets of paired states, there are the pair identity and smooth variation properties applicable for the energy levels, the wave functions, and the spectra $W^{(a)}_{L_1K_1K'_1}(\omega; j\tau)$ of states belonging to the same sets. This knowledge provides a useful hint for how to divide the H_2O lines into groups such that for lines in the same groups their calculated N_2 broadened half-widths have similar properties. It is obvious that in specifying the lines, one has to categorize their initial and final states simultaneously. First of all, in order to reduce one variable from j_i and j_f, one divides lines into the P, Q, and R branches. Then, by determining which of the sets of paired states their initial and final states belong to, one categorizes those lines in the same branches.

For example, a group in the R branch ($j_f = j_i + 1$) consists of a set of pairs of lines $\{j_{f0,j_f} \leftarrow j_{i1,j_i}, j_{f1,j_f} \leftarrow j_{i0,j_i}\}$ with $j_i = 0, 1, 2, \ldots$. In this group, two lines with the same j_i are called paired lines because their final sates j_{f0,j_f} and j_{f1,j_f} are paired partners in the same set and their initial states j_{i1,j_i} and j_{i0,j_i} are also paired partners in the same set. In this group, the pairs of lines are determined by only one variable j_i and the interesting pairs are those with j_i above the boundary j_{bd} (=7). Due to similar properties shared by their energy levels and wave functions, one expects that their calculated N_2-broadened half-widths must somehow follow a similarity too. In fact, for each of the paired lines in this group we have explicitly shown the spectra $W^{(a)}_{100}(\omega; j\tau)$ associated with their initial and final states in Figure 5(a) and provided their values of $P_{222}(j_f\tau_f j_i\tau_i)$ in Figure 10. Given the fact that the former mainly determine their $S_{2,\,outer,\,i}(r_c)$ and $S_{2,\,outer,\,f}(r_c)$ terms and the latter determine their $S_{2,\,middle}(r_c)$, one can be pretty sure that their half-widths must have similar properties. More specifically, as long as $j_i \geq 7$, the paired lines in this group should have the same half-width values. In addition, these values should vary smoothly with the pairs.

In order to demonstrate this claim, we present calculated $\mathrm{Re}S_2(r_c)$ at $T = 296\,\mathrm{K}$ for lines with $j_i = 7, 8, \ldots, 19$ in this group in Figure 12. The calculations are carried out with the modified RB formalism

Downloaded by [NASA Goddard Institute for Space Studies] at 07:23 23 April 2013

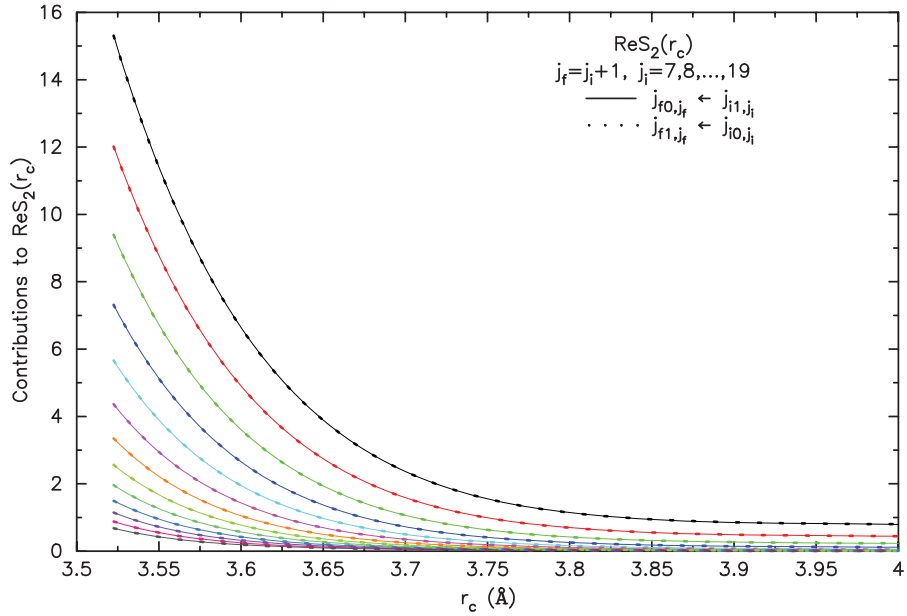

Figure 12. Calculated $\mathrm{Re}S_2(r_c)$ at $T = 296\,\mathrm{K}$ for lines with $j_i = 7, 8, \ldots, 19$ in the group of $j_{f0,j_f} \leftarrow j_{i1,j_i}$ and $j_{f1,j_f} \leftarrow j_{i0,j_i}$ in the R branch. For each of the paired lines, their $\mathrm{Re}S_2(r_c)$ are plotted by a solid and a dotted curves. Results associated with different j_i values are plotted by different colors and lie from top to bottom in the figure.

Downloaded by [NASA Goddard Institute for Space Studies] at 07:23 23 April 2013

and based on the potential model used in updating HITRAN 2008 [17]. In addition, 132 correlations have been taken into account and the 'exact' trajectory model was used. As shown in the figure, for each of the pairs their $\mathrm{Re}S_2(r_c)$ are always identical and the profiles of $\mathrm{Re}S_2(r_c)$ associated with different j_i values change very smoothly. Based on this, there are pair identity and smooth variation properties for their calculated half-widths because the latter are completely determined by these functions of $\mathrm{Re}S_2(r_c)$. We will return to this subject latter.

Similarly, one can define other groups in the R branch such as $\{j_{fn,j_f-n} \leftarrow j_{in+1,j_i-n}, j_{fn+1,j_f-n} \leftarrow j_{in,j_i-n}\}$ with $n = 1, 2, \ldots$. In defining these groups, values of k_c for their initial and final states are closer to the maxima. Meanwhile, we can define groups in the R branch where values of k_a are equal or close to the maxima, such as groups consisting of paired lines $\{j_{fj_f-n,n} \leftarrow j_{ij_i-n,n+1}, j_{fj_f-n,n+1} \leftarrow j_{ij_i-n,n}\}$ with $n = 0, 1, \ldots$. As long as the selection rule is allowed, more groups based on many other combinations of paired lines are accessible. In addition, there are groups consisting of un-paired lines. For example, $j_{fj_f-1,2} \leftarrow j_{i0,j_i}$ with $j_i = \mathrm{odd}$ are considered as un-paired lines because one cannot find other lines to pair both their final and initial states.

For the P and Q braches, one can perform similar procedures. As another example, we can define a group in the Q branch consisting of a set of paired lines $j_{f2,j_f-1} \leftarrow j_{i1,j_i}$ and $j_{f1,j_f-1} \leftarrow j_{i0,j_i}$ with $j_i = 1, 2, \ldots$. We present calculated $\mathrm{Re}S_2(r_c)$ at $T = 296\,\mathrm{K}$ for pairs of lines with $j_i = 9, 10, \ldots, 20$ in this group in Figure 13. As shown in the figure, profiles of these functions of $\mathrm{Re}S_2(r_c)$ have similar features as the group in the R branch given above.

6. Pair identity and smooth variation rules for the half-widths

After categorizing H_2O lines based on properties of energy levels and wave functions of their initial and final states, we are ready to establish rules applicable for the calculated half-widths for lines within individual groups.

We select six groups of lines in the pure rotational band and present their calculated N_2-broadened half-widths in Figure 14(a–f). They are three groups of $\{j_{f0,j_f} \leftarrow j_{i1,j_i}, j_{f1,j_f} \leftarrow j_{i0,j_i}\}$, $\{j_{f1,j_f-1} \leftarrow j_{i2,j_i-1}, j_{f2,j_f-1} \leftarrow j_{i1,j_i-1}\}$, and $\{j_{f2,j_f-2} \leftarrow j_{i1,j_i}, j_{f3,j_f-2} \leftarrow j_{i0,j_i}\}$ in the R branch, two groups of $\{j_{f1,j_f-1} \leftarrow j_{i0,j_i}, j_{f2,j_f-1} \leftarrow j_{i1,j_i}\}$ and $\{j_{f2,j_f-2} \leftarrow j_{i1,j_i-1}, j_{f3,j_f-2} \leftarrow j_{i2,j_i-1}\}$ in the Q branch, and one group of $\{j_{f2,j_f-2} \leftarrow j_{i1,j_i}, j_{f3,j_f-2} \leftarrow j_{i0,j_i}\}$ in the P branch. As shown in the figures, paired lines with their j_i values above boundaries in all six groups have almost identical half-widths. In addition, by comparing different pairs in the same groups, their half-widths vary smoothly as their j_i values vary. In general, the boundaries of the groups of lines are determined by

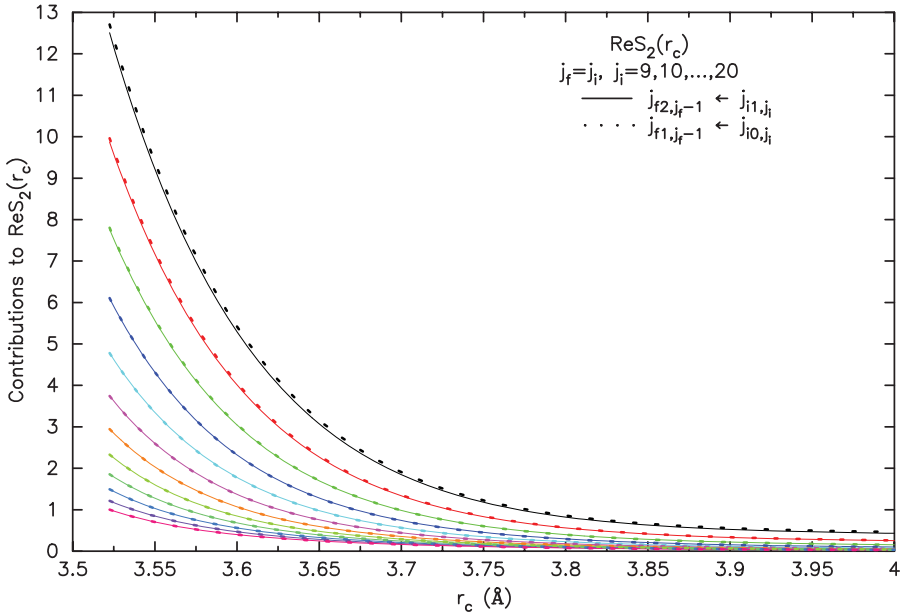

Figure 13. The same as Figure 12 except for lines with $j_i = 9, 10, \ldots, 20$ in a group of $j_{f2,j_f-1} \leftarrow j_{i1,j_i}$ and $j_{f1,j_f-1} \leftarrow j_{i0,j_i}$ in the Q branch.

states with the smallest of $|k_a - k_c|$. With Table 2, one can predict these boundaries and they are 7, 10, 13, 10, 13, and 14, respectively. We note that for lines in the P branch, their j_f are less than j_i. As a result, the boundary requirement applies for j_f (i.e. $j_f \geq 13$) and the latter means $j_i \geq 14$.

Thus, the pair identity and smooth variation rules applicable for calculated half-widths for lines involving high j states within the groups can be established. The higher the j_i, the firmer these two rules hold. As explained above, the very origin of these two rules is the properties of the energy levels and the wave functions of H_2O states. No matter what kinds of potential and trajectory models are used in calculations, theoretically calculated N_2-broadened half-widths must follow these rules.

Furthermore, by scrutinizing the whole process presented above, one cannot find any reason why the analyzing process and the final conclusions described above for the widths are not applicable for calculated pressure-induced shifts. In fact, with the modified RB formalism, the expression for the shift is given by

$$\delta_{MRB} = \frac{n_b}{2\pi c}\int_0^{+\infty} \nu f(\nu)\mathrm{d}\nu \int_0^{+\infty} 2\pi b db \sin(\langle S_1(b)\rangle + \mathrm{Im}\langle S_2(b)\rangle)e^{-\mathrm{Re}\langle S_2(b)\rangle}. \quad (33)$$

For lines in the pure rotational band, by replacing the integration over the velocity by the averaged velocity the above expression can be simplified as

$$\delta_{MRB} = \frac{n_b \bar{v}}{2\pi c}\int_{r_{c,\min}}^{+\infty} 2\pi b\left(\frac{\mathrm{d}b}{\mathrm{d}r_c}\right)\sin[\mathrm{Im}S_2(r_c)]e^{-\mathrm{Re}S_2(r_c)}\mathrm{d}r_c. \quad (34)$$

Because $S_{2,\,middle}(r_c)$ is real, $\mathrm{Im}S_2(r_c)$ consists of only two components $-\mathrm{Im}S_{2,\,outer,\,i}(r_c)$ and $\mathrm{Im}S_{2,\,outer,\,f}(r_c)$ where the minus sign of $\mathrm{Im}S_{2,\,outer,\,i}(r_c)$ results from the fact that $S_2(r_c) = S_{2,\,outer,\,i}(r_c)^* + S_{2,\,outer,\,f}(r_c) + S_{2,\,middle}(r_c)$ [11]. The expression for $\mathrm{Im}S_{2,\,outer,\,i}(r_c)$ is the same as Equation (9) for $\mathrm{Re}S_{2,\,outer,\,i}(r_c)$ except for a replacement of $H_{L_1K_1K_1'L_2}(\omega)$ by the Cauchy principal integrations $I_{L_1K_1K_1'L_2}(\omega)$ defined by

$$I_{L_1K_1K_1'L_2}(\omega) = -\frac{1}{\pi}P\int_{-\infty}^{+\infty}\mathrm{d}\omega'\frac{1}{\omega'-\omega}H_{L_1K_1K_1'L_2}(\omega'), \quad (35)$$

where P means the principal part. Similar to the function of $H_{L_1K_1K_1'L_2}(\omega)$, $I_{L_1K_1K_1'L_2}(\omega)$ are common for all lines. As a result, all the discussions given above are applicable for the calculated shifts and the same two rules must be valid also.

One can extend the discussions to other temperatures for the H_2O–N_2 system. One can carry out similar analysis for other systems involving different perturbers such as H_2O–O_2 and H_2O–H_2O. It seems that there are no any essential differences occurring among these different cases. Therefore, the two rules are not

Downloaded by [NASA Goddard Institute for Space Studies] at 07:23 23 April 2013

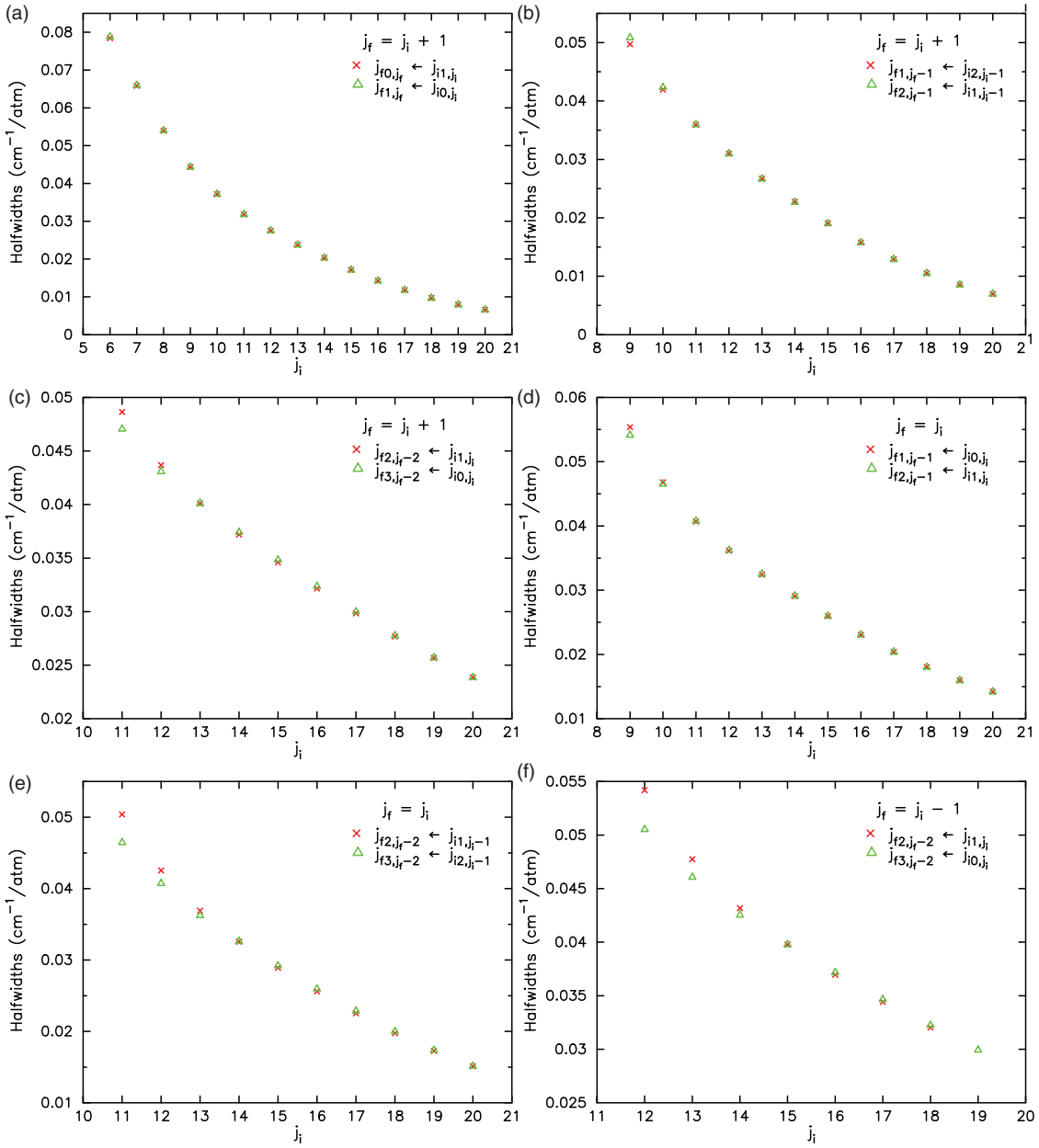

Figure 14. Calculated N_2-broadened half-widths for paired H_2O lines in six groups defined in the pure rotational band. Three groups in the *R* branch are plotted in (a)–(c), two groups in the *Q* branch are in (d)–(e), and one group in the *P* branch is in (f).

Downloaded by [NASA Goddard Institute for Space Studies] at 07:23 23 April 2013

only applicable for the N_2-broadened half-widths, but also for the air- and self-broadened half-widths and their corresponding temperature exponents.

7. Discussion and conclusions

Based on this understanding acquired in the present study, one can develop useful ways to improve the accuracy of the spectroscopic parameters in databases. First of all, by applying the identity rule to two paired lines, one is able to pick out those values listed in the database that differ appreciably from one another. One can be fairly sure that those data picked out contain large errors or, for instance, came from different theoretical or experimental sources. Meanwhile, by applying the smooth variation rule for lines in the same groups, their individual errors could be partially averaged out using proper smoothing procedures. Thus, one is able to obtain better values with less uncertainty.

Downloaded by [NASA Goddard Institute for Space Studies] at 07:23 23 April 2013

For people who are in charge of databases, the present work provides a helpful guide and a useful tool in their developing practices. It is wise to consider that all lines in each of the transition bands belong to a well organized network. Acting as one member of the network, the half-width value of an individual line is not self-contained because it has to be somehow connected with other values associated with those lines, especially its paired line, who belong to the same group as the line of interest does. The same statement is also true for other spectroscopic parameters. Given the fact that data listed in the databases may come from several independent sources, to take a balance procedure becomes even necessary. Meanwhile, by applying the two rules to each of the groups of lines thoroughly, one can screen the database and identify lines whose half-width values (or other spectroscopic parameters) that behave strangely. These outliers should be carefully checked, or one could consider the option to replace them by smoothed values obtained from their neighboring lines. After removing the errors, they are able to improve the accuracy of the database significantly.

Experimentalists can also use the pair identity and smooth variation rules to check their measured spectroscopic data. If their results scatter wildly, it definitely indicates contaminations or errors existing in their data. In addition, the smooth variation rule provides a sound support and is a useful guide for their developing data smoothing procedures. Again, one has to keep in mind that although the smoothing practice for data with high j states in the same groups is well justified, one cannot apply it to those lines with low j states, otherwise the procedures could introduce artificial errors. Finally, with respect to the determination of measurement priorities, it is prudent to choose several lines with high js in the same group because several good measurements are enough to determine others in the same group. This implies that it is not necessary to measure all lines in the same group for the completeness purpose.

In summary, it is the properties of energy levels and wave functions of the H_2O states that play an essential role in establishing the pair identity and the smooth variation rules and these rules reflect natural correlations between the inputs and the outputs for a whole system consisting of an absorber H_2O molecule immersed in bath molecules and radiation fields. However, due to the complexity of dynamical processes happening inside the system, these correlations are very difficult to be fully grasped. This implies that it is unrealistic to set as a goal to find common rules with which the outputs can be well monitored from the inputs unless one narrows the variation range of the inputs. Thus, it is the categorization of the H_2O lines that enable one to narrow the variation ranges of the inputs first. In fact, after completing the categorization procedures for each of the P, Q, and R branches, there is only one independent variable (i.e. the initial quantum number j_i) left to distinguish lines of interest. Then to establish the rules valid within the individual groups becomes possible. Therefore, these two rules have two characteristics: they are natural, but they are local. Local here means the rules work for each individual groups and are valid only for its members above certain boundaries. Finally, while the present study was carried out in the pure rotational band of H_2O, one can extend the study to other H_2O bands and establish similar rules there also. Of course, one has to analyse the properties of the energy levels and wave functions of the states involved in these transitions first.

Acknowledgements

Two of the authors (Q. Ma and R.H. Tipping) acknowledge financial support from NASA under grants NNG06GB23G, NNX09AB62G, and FCCS-547. Q. Ma wishes to acknowledge financial support from the Biological and Environmental Research Program (BER), US Department of Energy, Interagency Agreement No. DE-AI02-93ER61744 and financial support from NASA under grant NNH08ZDA001N-ACLAB. This research used resources of the National Energy Research Scientific Computing Center, which is supported by the Office of Science of the U.S. Department of Energy under Contract No. DE-AC02-05CH11231.

References

[1] L.S. Rothman, I.E. Gordon, A. Barbe, D.C. Benner, P.F. Bernath, M. Birk, V. Boudon, L.R. Brown, A. Campargue, J.-P. Champion, K. Chance, L.H. Coudert, V. Dana, V.M. Devi, S. Fally, J.-M. Flaud, R.R. Gamache, A. Goldman, D. Jacquemart, I. Kleiner, N. Lacome, W.J. Lafferty, J.-Y. Mandin, S.T. Massie, S.N. Mikhailenko, C.E. Miller, N. Moazzen-Ahmadi, O. Naumenko, A.V. Nikitin, J. Orphal, V.I. Perevalov, A. Perrin, A. Predoi-Cross, C.P. Rinsland, M. Rotger, M. Simecková, M.A.H. Smith, K. Sung, S.A. Tashkun, J. Tennyson, R.A. Toth, A.C. Vandaele and J. Vander Auwera, J. Quant. Spectrosc. Radiat. Transfer **110**, 533 (2009).

[2] I.E. Gordon, L.S. Rothman, R.R. Gamache, D. Jacquemart, C. Boone, P.F. Bernath, M.W. Shephard, J.S. Delamore and S.A. Clough, J. Quant. Spectrosc. Radiat. Transfer **108**, 389 (2007).

[3] D. Robert and J. Bonamy, J. Phys. (France) **40**, 923 (1979).

[4] Q. Ma, R.H. Tipping and R.R. Gamache, Mol. Phys. **108**, 2225 (2010).
[5] Q. Ma, R.H. Tipping and N.N. Lavrentieva, Mol. Phys. **109**, 1925 (2011).
[6] G.W. King, R.M. Hainer and P.C. Cross, J. Chem. Phys. **11**, 27 (1943).
[7] H.C. Allen and P.C. Cross, *Molecular Vib-Rotors* (Wiley, New York, 1963).
[8] W. Gordy and R.L. Cook, *Microwave Molecular Spectra* (Wiley, New York, 1970).
[9] R.N. Zare, *Angular Momentum* (Wiley, New York, 1988).
[10] R.J. Barber, J. Tennyson, G.H. Harris and R.N. Tolchenov, Mon. Not. R. Astron. Soc. **368**, 1087 (2006).
[11] R. Lynch, R.R. Gamache and S.P. Neshyba, J. Chem. Phys. **105**, 5711 (1996).
[12] R.R. Gamache and J. Fischer, JQSRT **78**, 289 (2003); **78**, 305 (2003).
[13] R.R. Gamache and J.-M. Hartmann, J. Can. Chem. **82**, 1013 (2004).
[14] R.R. Gamache, J. Mol. Spec. **229**, 9 (2005).
[15] Q. Ma, R.H. Tipping and C. Boulet, J. Quant. Spectrosc. Radiat. Transfer **103**, 588 (2007).
[16] Q. Ma, R.H. Tipping and C. Boulet , J. Chem. Phys. **124**, 014109 (2006).
[17] R.R. Gamache and A. Laraia, J. Mol. Spectrosc. **257**, 116 (2009).

Downloaded by [NASA Goddard Institute for Space Studies] at 07:23 23 April 2013

Appendix

A.1. Symmetry assignments of H_2O wave functions for paired states

We consider the symmetry assignments for the sets of paired states $j_{j-n,n}$ and $j_{j-n,n+1}$ where $n=0,1,\ldots$ whose wave functions in the I R representation are given in Figure 2. It is obvious that the paired states have the same k_a values, but their k_c values differ from each other by 1. This implies that they have identical evenness or oddness for k_a, but have opposite evenness or oddness for k_c. Thus according to Table 1, no matter whether their j values are even or odd, their symmetry assignments by the superscripts + and − in the I R representation must be opposite. In terms of their coefficients $U^j_{k\tau}$, the coefficients of one state must be an even function of k and the coefficients of its paired partner must be an odd function of k. In Table A-1, we list the assignments for these pairs.

Table A-1 Symmetry assignments for pairs of $j_{j-n,n}$ and $j_{j-n,n+1}$ in the I R representation.

	$j_{j,0}, j_{j,1}$	$j_{j-1,1}, j_{j-1,2}$	$j_{j-2,2}, j_{j-2,3}$	⋯
$j=$ even	E^+, E^-	O^+, O^-	E^+, E^-	
$j=$ odd	O^+, O^-	E^+, E^-	O^+, O^-	

Similarly, we consider the symmetry assignments for the sets of paired states $j_{n,j-n}$ and $j_{n+1,j-n}$ where $n=0,1,\ldots$ whose wave functions in the III R representation are given in Figure 3. In this case, the paired states have the same k_c and their k_a differ from each other by 1. Then, one can conclude that with respect to their wave functions derived in the III R representation, one must be an even function assigned by the superscript + and its partner must be an odd function assigned by the superscript −. In terms of their coefficients $U^j_{k\tau}$, the conclusion is the same as that for the sets of $j_{j-n,n}$ and $j_{j-n,n+1}$ drawn above. In Table A-2, we list the assignments for them. These symmetry properties are important and we will be back to this subject later.

A.2. Important quantities in determining couplings between H_2O states

As shown in Section 4, in the RB formalism there are two quantities which play crucial roles in determining how the Lorentzian half-widths would vary with lines of interest. For two H_2O states $j\tau$ and $j'\tau'$ which can be coupled by the irreducible tensor L and its subsidiary index K, the quantities $\omega_{j\tau j'\tau'}$ defined by

$$\omega_{j\tau j'\tau'} = [E^{(H_2O)}(j\tau) - E^{(H_2O)}(j'\tau')]/\hbar \qquad \text{(A-1)}$$

represent their energy differences and the quantities $D(j\tau j'\tau'; LK)$ called as the D matrices represent their couplings; and this is defined by

$$D(j\tau j'\tau'; LK) = \sum_k (-1)^k U^j_{k\tau} U^{j'}_{k-K\tau'} C(jj'L, kK-kK). \qquad \text{(A-2)}$$

As shown by Equation (A-1) and (A-2), with the energy levels and the wave functions of these two states, one can easily calculate the energy differences and the D matrices.

However, it turns out that exploiting the properties of these two quantities is fruitful in answering a fundamental question why and how the calculated N_2-broadened half-widths and pressure induced shifts would vary with lines of interest. Based on our analysis of the properties of the energy levels and the wave functions of the H_2O described previously, one can find the properties of these two quantities accordingly.

Let us consider two pairs of the states $\{j\,\tau_1, j\,\tau_2\}$ and $\{j'\,\tau'_1, j'\,\tau'_2\}$. We assume $j\,\tau_1$ and $j\,\tau_2$ are paired and $j'\,\tau'_1$ and $j'\,\tau'_2$ are paired. By picking one member from each of the pairs, one gets two combinations, for example, a combination of $j\,\tau_1$ and $j'\,\tau'_1$ and a combination of $j\,\tau_2$ and $j'\,\tau'_2$. We assume that the two states in the same combinations can be coupled by L and K where L is the irreducible tensor rank and K is its associated index [4,16], and we would like to compare the energy differences and the D matrices between these two

Table A-2. Symmetry assignments for pairs of $j_{n,j-n}$ and $j_{n+1,j-n}$ in the III R representation.

	$j_{0,j}, j_{1,j}$	$j_{1,j-1}, j_{2,j-1}$	$j_{2,j-2}, j_{3,j-2}$	⋯
$j=$ even	E^+, E^-	O^-, O^+	E^+, E^-	
$j=$ odd	O^-, O^+	E^+, E^-	O^-, O^+	

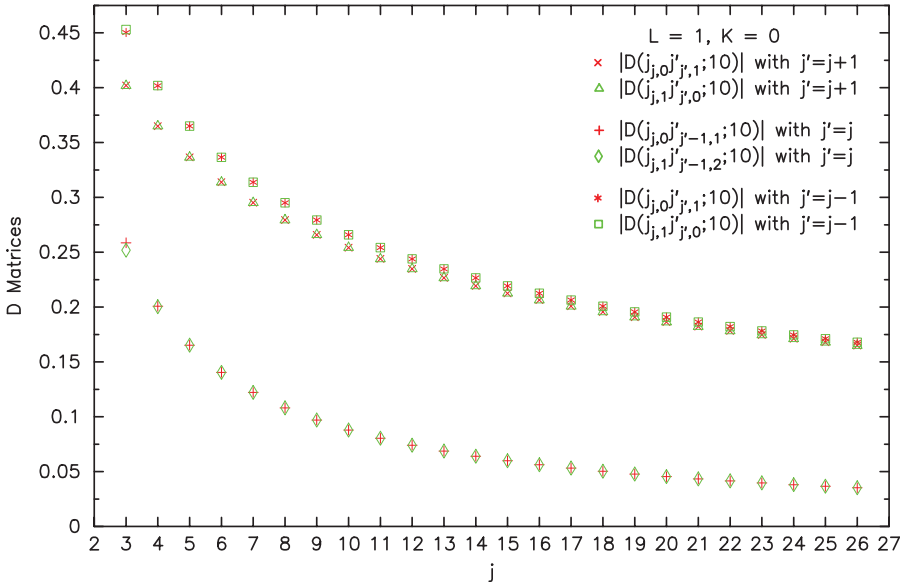

Figure A.1. A plot to show properties of $D(j_{k_a,k_c}j'_{k'_a,k'_c};LK)$ with $L=1$ and $K=0$. Calculated values of $|D(j_{j,0}j'_{j',1};10)|$ and $|D(j_{j,1}j'_{j',0};10)|$ with $j'=j+1$ and $j=3,\ldots 26$ are plotted by $\times$ and Δ, respectively. Because values are positive for even j and become negative for odd j. In order to show how their magnitudes vary with j more clearly, their absolute values are plotted in the figure. Similarly, a set of pairs $|D(j_{j,0}j'_{j'-1,1};10)|$ and $|D(j_{j,1}j'_{j'-1,2};10)|$ with $j'=j$ whose values are negative for even j and positive for odd j are plotted by $+$ and $\Diamond$. Finally, another set of pairs $|D(j_{j,0}j'_{j',1};10)|$ and $|D(j_{j,1}j'_{j',0};10)|$ with $j'=j-1$ whose values are negative for even j and positive for odd j are plotted by * and $\square$.

combinations. First of all, it is obvious that there are identities of their energy differences

$$\omega_{j\tau_1 j'\tau'_1} \approx \omega_{j\tau_2 j'\tau'_2} \tag{A-3}$$

approximately valid within certain accuracy tolerances when both j and j' are above corresponding boundaries defined for their sets.

On the other hand, for the two D matrices $D(j\tau_1 j'\tau'_1;LK)$ and $D(j\tau_2 j'\tau'_2;LK)$, one has shown that $|U^j_{k\tau_1}| \approx |U^j_{k\tau_2}|$ and $|U^{j'}_{k\tau'_1}| \approx |U^{j'}_{k\tau'_2}|$. In addition, as shown in Section A.1, the evenness or oddness of $U^j_{k\tau_1}$ and $U^j_{k\tau_2}$ over k must be opposite and this is true for $U^{j'}_{k\tau'_1}$ and $U^{j'}_{k\tau'_2}$ also. Thus, it becomes clear that

$$U^j_{k\tau_1}\, U^{j'}_{k-K\tau_1} \approx U^j_{k\tau_2}\, U^{j'}_{k-K\tau'_2}. \tag{A-4}$$

As a result, one is able analytically to verify

$$D(j\tau_1 j'\tau'_1;LK) \approx D(j\tau_2 j'\tau'_2;LK). \tag{A-5}$$

Thus, one can draw an important conclusion that the coupling by L and K between two states approximately equals the coupling between their paired partners. The higher the j is, the more equal these couplings become. We call these two D matrices as the paired D matrices later. Besides, there is another interesting feature of the paired D matrices. This feature represents a behavior of their values as j varies. In order to exhibit it, one has to find their values by performing numerical calculations explicitly.

It is worth mentioning that Equation (A-4) is applicable for the coefficients derived accordingly in the I R or III R representation, but not in the II R representation. This implies that we have verified Equation (A-5) analytically in the I R and III R representations, but not in the II R representation. On the other hand, in developing the line shape formalism with the correlation functions described in Section 3, we prefer to choose the II R representation in which the symmetry axis of the H_2O molecule lies along the z axis of the molecular fixed frame. With this choice, one is able to exploit more symmetries of H_2O to reduce a number of the correlation functions required to be evaluated significantly. Because Equation (A-4) is not valid, to verify Equation (A-5) analytically in the II R representation is not as easy as shown above. In the present study, we do not pursue the analytical verification, rather we carry out numerical verification. In addition, numerical results are needed to exhibit another feature of the paired D matrices.

For later convenience, we rewrite $D(j\tau j'\tau';LK)$ as $D(j_{k_a,k_c}j'_{k'_a,k'_c};LK)$ where $k_a-k_c=\tau$ and $k'_a-k'_c=\tau'$. We note that there are rules to determine whether there are non-zero couplings between two states j_{k_a,k_c} and $j'_{k'_a,k'_c}$ or not. For example, in the II R representation the rule associated with $L=1$ and $K=0$ is similar to the selection rule of the H_2O transitions; Δj $(\equiv j'-\mathrm{j})=0,\pm 1$, Δk_a $(\equiv k'_a-k_a)=\pm 1,\pm 3,\ldots$, and Δk_c $(\equiv k'_c-k_c)=\pm 1,\pm 3,\ldots$. The rule for $L=2$ and $K=0$ is $\Delta j=0,\pm 1,\pm 2$, $\Delta k_a=0,\pm 2,\pm 4,\ldots$, and $\Delta k_c=0,\pm 2,\pm 4,\ldots$. For other L and K values, the rules become more complicated.

As an example, we consider a set of two D matrices $\{D(j_{j,0}j'_{j',1};10), D(j_{j,1}j'_{j',0};10)\}$ with $j'=j+1$. It is obvious that these two are paired D matrices because $j_{j,0}$ of the first D and $j_{j,1}$ of the second D are paired states, and $j'_{j',1}$ in the fist D and $j'_{j',0}$ in the second D are paired. In addition, there are non-zero couplings both between $j_{j,0}$ and $j'_{j',1}$ of the first D and between $j_{j,1}$ and $j'_{j',0}$ of the second D. We have calculated these two paired D matrices for values of for $j=3,\ldots 26$ and

Downloaded by [NASA Goddard Institute for Space Studies] at 07:23 23 April 2013

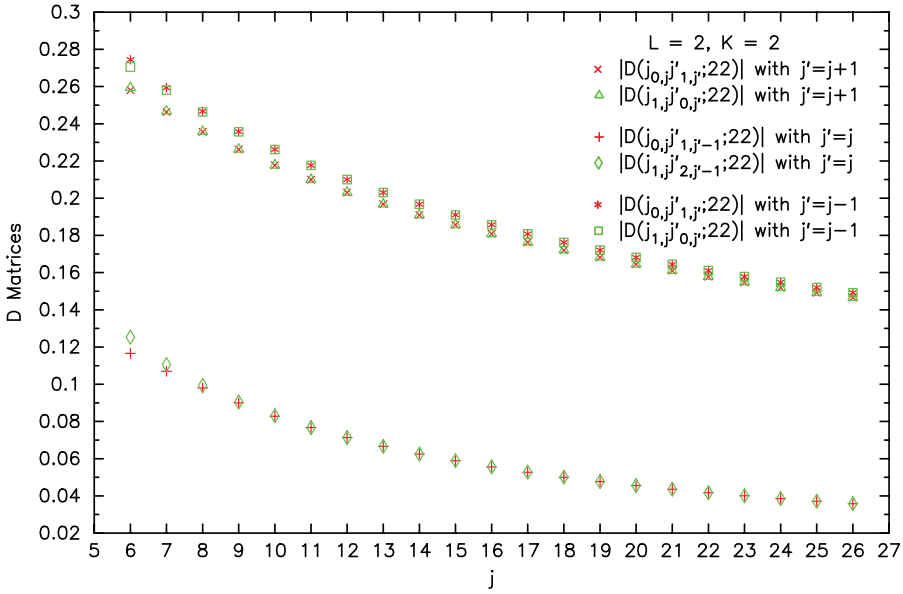

Figure A.2. The same as Figure A.1 except for $L=2$, $K=2$, three sets of the paired D matrices $\{D(j_{0,j}j'_{1,j'};22), D(j_{1,j}j'_{0,j'};22)\}$ with $j'=j+1$, $\{D(j_{0,j}j'_{1,j'-1};22), D(j_{1,j}j'_{2,j'-1};22)\}$ with $j'=j$, and $\{D(j_{0,j}j'_{1,j'};22), D(j_{1,j}j'_{0,j'};22)\}$ with $j'=j-1$.

found their values are almost identical. However, it turns out that the values are positive for $j=$even and become negative for $j=$odd. In order to show how their magnitudes vary with j more clearly, we plot their calculated magnitudes in Figure A-1. Similarly, we select another two sets $\{D(j_{j,0}j'_{j'-1,1};10), D(j_{j,1}j'_{j'-1,2};10)\}$ with $j'=j$ and $\{D(j_{j,0}j'_{j',1};10), D(j_{j,1}j'_{j',0};10)\}$ with $j'=j-1$. Both of them have non-zero couplings and both of them consist of two paired D matrices. Again, because their calculated values change signs for even j and odd j alternatively, we plot their magnitudes in Figure A.1. Based on these results, we can draw two conclusions. First of all, values of the paired D matrices are almost identical. This implies that we have verified Equation (A-5) numerically for these sets. In addition, we would like to note that for these three sets, the identity of paired D matrices becomes valid starting from $j=3$, 5, and 4, respectively. These j values are consistent with those j_{bd} values listed in Table 2. Readers may wonder for the third set, why the identity starts from $j=4$, but not $j=3$. It is easy to explain this because for this set, $j'=j-1$ and the smaller of j and j' must be not less j_{bd}. Secondly, as shown in the figure, one can conclude that for each of these sets, their magnitudes vary very smoothly as j varies. Variation of the magnitudes with j smoothly is just a feature of the paired D matrices we are looking for.

As another example, instead of choosing states associated with large k_a values we consider sets of the paired D matrices whose states are associated with large k_c values. In addition, with respect to L and K we consider a case of $L=2$ and $K=2$. More specifically, we select $\{D(j_{0,j}j'_{1,j'};22), D(j_{1,j}j'_{0,j'};22)\}$ with $j'=j+1$, $\{D(j_{0,j}j'_{1,j'-1};22), D(j_{1,j}j'_{2,j'-1};22)\}$ with $j'=j$, $\{D(j_{0,j}j'_{1,j'};22), D(j_{1,j}j'_{0,j'};22)\}$ with $j'=j-1$. We present their calculated magnitudes with $j=5,\ldots 26$ in Figure A.2. As shown in the figure, the two features exhibited previously remain the same. We do not repeat the discussion here, other than to mention that in comparison with the previous three sets, the identity of two paired D becomes valid starting from a higher j value. For these three sets, it starts from $j=7$, 10, and 8, respectively. These starting values are consistent with those j_{bd} values listed in Table 2.

With respect to other sets, we believe the same conclusions mentioned above are applicable there also. As shown in Section 3 these two features of the paired D matrices are very helpful in analyzing values of calculated half-width for the H_2O lines.

Downloaded by [NASA Goddard Institute for Space Studies] at 07:23 23 April 2013